

Causal inference with outcome dependent sampling and mismeasured outcome

Min Zeng¹, Zeyang Jia¹, Zijian Sui¹, Jinfeng Xu^{2,*}, and Hong Zhang^{1,**}

¹Department of Statistics and Finance, University of Science and Technology of China, Anhui, China

²Department of Biostatistics, City University of Hong Kong, Hong Kong, China.

**email*: jinfenxu@cityu.edu.hk

***email*: zhangh@ustc.edu.cn

SUMMARY: Outcome-dependent sampling designs are extensively utilized in various scientific disciplines, including epidemiology, ecology, and economics, with retrospective case-control studies being specific examples of such designs. Additionally, if the outcome used for sample selection is also mismeasured, then it is even more challenging to estimate the average treatment effect (ATE) accurately. To our knowledge, no existing method can address these two issues simultaneously. In this paper, we establish the identifiability of ATE and propose a novel method for estimating ATE in the context of generalized linear model. The estimator is shown to be consistent under some regularity conditions. To relax the model assumption, we also consider generalized additive model. We propose to estimate ATE using penalized B-splines and establish asymptotic properties for the proposed estimator. Our methods are evaluated through extensive simulation studies and the application to a dataset from the UK Biobank, with alcohol intake as the treatment and gout as the outcome.

KEY WORDS: Average treatment effect; Causal inference; Outcome dependent sampling; Outcome mismeasurement.

1. Introduction

Numerous studies in the fields of biomedical and social sciences are focused on determining the causal impact of a binary treatment on a specific outcome. Although randomized controlled trials (RCTs) serve as the gold standard for establishing causal relationships, they may not always be feasible due to financial, logistical, or ethical constraints. As a result, researchers often rely on observational studies. Various methodologies, such as propensity score techniques (Rosenbaum and Rubin, 1983; Rubin and Thomas, 2000) and instrumental variable estimation methods (Angrist et al., 1996; Angrist and Krueger, 2001), have been developed to estimate average treatment effect (ATE) in observational studies. However, the efficacy of these methodologies relies on sampling randomness. In cases where sample selection is not random, these methods are no longer valid.

Outcome-dependent sampling (ODS) represents a non-random sampling design in which the selection of sample units depends on the outcome of interest. ODS offers some advantages over simple random sampling, such as enhanced statistical power in the situation where the outcome is rare (Schlesselman, 1982). However, ODS greatly complicates the statistical data analysis and result interpretation. The case-control design, along with its variations, is the most prevalent form of ODS design. Ideally, in such designs, the sampling process relies exclusively on the outcome rather than any other variables in the study. If the unique characteristics of ODS designs are not considered, the conventional causal inference methods may be subject to selection bias (Gabriel et al., 2022; Bareinboim and Pearl, 2016). A large quantity of research based on ODS designs has been published (Wacholder et al., 1992; Breslow and Holubkov, 1997), but the majority of these studies focus on association analysis instead of causal inference. Several researchers (L. Penning de Vries and Groenwold, 2022; Månsson et al., 2007; Robins, 1999) have attempted to avoid this issue by focusing on causal risk ratio. Van der Laan (2008) and Van der Laan and Rose (2011), on the other

hand, proposed an ATE estimator based on a weighted targeted maximum likelihood by incorporating information on disease prevalence.

However, implementing an ideal ODS design in practice can often be challenging, as sample selection may be influenced, at least partially, by diagnosis or measurement. As a result, the true outcome of interest may be unobserved, and the measured outcome may differ from the true outcome. Various factors contribute to mismeasurement in outcome variables, such as the unavailability of costly measurements, the propensity to misreport responses to sensitive questions, and the inevitable recall bias. Numerous studies have investigated the impact of mismeasurement of outcome variables such as bias and efficiency loss (Copeland et al., 1977; Neuhaus, 1999; Shu and Yi, 2019a; Fox et al., 2022). Some researchers have opted to develop sensitivity analyses of mismeasured binary outcomes to reduce bias (Lash and Fink, 2003; Fox et al., 2005; Lyles and Lin, 2010). Shu and Yi (2019a, 2020, 2019b) derived asymptotic bias of the conventional inverse probability of treatment weighting (IPTW) and doubly robust (DR) estimators ignoring the measurement error, and proposed a modified weighting method by rectifying the mismeasurement bias.

Although research on addressing either selection bias or mismeasurement bias has garnered much attention, very few methods have been developed to deal with these two types of bias simultaneously except for Beesley and Mukherjee (2022) and Jurek et al. (2013). However, these studies focus on association analysis. To our knowledge, no causal inference method has been developed to simultaneously address both issues. In this paper, we derived a novel generalized linear model (GLM) to establish the relationship between the observed samples and the target population. This allows for an intuitive understanding of the combined effects of ODS and measurement error on ATE estimation. Then we derive estimation equations (EE) to estimate unknown parameters, through which we obtain an ATE estimator. We call this method GLM-EE. The GLM-EE estimator is proven to be consistent and asymptotically

normal. Furthermore, to relax model assumption, we introduce a generalized additive model (GAM) based estimator (Hastie and Tibshirani, 1987; Yoshida and Naito, 2014; Marx and Eilers, 1998), which employs penalized spline as a smoothing technique. Unknown parameters can again be estimated by solving a set of estimation equations and we refer to this method as GAM-EE. Asymptotic properties of the GAM-EE estimator are also established. Through simulation study, we demonstrate that both proposed estimators effectively address selection bias and mismeasurement bias. Moreover, the GAM-EE method is shown to be more robust to model misspecification with little efficiency sacrifice.

We further applied our method to a real-world dataset from the UK Biobank, which aims to investigate the ATE of alcohol consumption (treatment) on gout disease (outcome) among male individuals aged 40 to 80. Gout is a form of arthritis that arises when uric acid crystals accumulate in the joints, causing inflammation and pain. However, this outcome measurement suffers from misdiagnoses with a high false negative rate of 10-30% and a low false positive rate of about 5% (Vázquez-Mellado et al., 2012; Kiefer et al., 2016). We applied our methods to this dataset and conducted a sensitivity analysis to evaluate their performance in real-world research.

The remainder of this article is structured as follows. In Section 2, we introduce our model and establish the identifiability of ATE under some appropriate assumptions. In Section 3, we describe our GLM-EE and GAM-EE methods and establish their theoretical properties. In Section 4 and Section 5, we evaluate the performance of the two methods through extensive simulation studies and a real data application, respectively. In Section 6, we conclude the article and discuss future research directions. All technical details, along with supplementary information for the numerical studies in Sections 4 and 5, are provided in Supplementary Materials.

2. Identifiability of average treatment effect

2.1 Ordinary scenario

We start by reviewing the identifiability of ATE in ordinary scenarios where samples are selected randomly and measurement error is absent. Let T and Y denote the binary treatment and true outcome of interest, respectively. Let $Y(t)$ denote the potential or counterfactual outcome for a given subject with exposure level t (Rubin, 2005). Suppose Y , T , and $Y(t)$ take values in the binary set $\{0, 1\}$. Let X denote a vector of covariates or confounding variables. Our target parameter ATE, denoted as τ , is defined as the expected difference between the potential outcomes:

$$\tau = \mathbb{E}[Y(1) - Y(0)],$$

where the expectation is evaluated in the target population.

In the standard causal inference framework, the identifiability of τ hinges on three fundamental assumptions stated as follows:

ASSUMPTION 1: (consistency)

$$Y = TY(1) + (1 - T)Y(0).$$

ASSUMPTION 2: (positivity)

$$1 > \mathbb{P}(T = 1|X) > 0.$$

ASSUMPTION 3: (unconfoundness)

$$(Y(1), Y(0)) \perp T \mid X.$$

Under Assumptions 1-3, τ is identifiable, as demonstrated by the following formula:

$$\tau = \mathbb{E}\{g_1(X) - g_0(X)\}, \tag{1}$$

where $g_i(x) = \mathbb{E}[Y \mid X = x, T = i]$, $i = 1, 0$.

As evident from Equation (1), the identifiability of τ relies not only on g_1 and g_0 but also on

the distribution of covariates X in the target population. In scenarios involving ODS designs and measurement error, both $g_i(x)$ and the distribution of X are ambiguous. Consequently, the identifiability of τ needs further assumptions.

2.2 ODS with measurement error

Let Y^* denote the observed outcome, which may differ from the true outcome Y due to measurement error. Let S represent an indicator of selection into the study, with $S = 1$ for “selected” and $S = 0$ for “not selected”. The sample distribution is expressed by $\mathbb{P}(Y^*, X, T | S = 1)$, where $\mathbb{P}(\cdot)$ denotes the probability density function. To ensure the identifiability of τ , we introduce two additional assumptions characterizing the mechanism of sample selection and outcome measurement.

ASSUMPTION 4: (selection conditional independence): the sample selection procedure is independent of (Y, X, T) given Y^* , that is

$$S \perp (Y, X, T) | Y^*.$$

ASSUMPTION 5: (measurement conditional independence): the observed outcome Y^* is independent of (X, T) given Y , that is

$$Y^* \perp (X, T) | Y.$$

Assumption 4 naturally aligns with outcome-dependent sampling (ODS) design, as it posits that samples are selected solely based on the observed outcome Y^* . Assumption 5 states that the observed outcome Y^* relies exclusively on the true outcome Y , which indicates the influence of X and T on Y^* is completely mediated by Y . This frequently arises in clinical diagnosis and is extensively employed in the literature (Shu and Yi, 2019a, 2020). Figure 1 employs the directed acyclic graph (DAG) to illustrate the problem, where subfigure (a) corresponds to the ordinary design under Assumptions 1-3, while subfigure (b) depicts the ODS design with measurement error under Assumptions 1-5.

[Figure 1 about here.]

It follows from Assumptions 4 and 5 that $\mathbb{P}(Y^* = j | Y = i, X) = \mathbb{P}(Y^* = j | Y = i)$ and $\mathbb{P}(S = j | Y^* = i, X) = \mathbb{P}(S = j | Y^* = i)$ for $i, j = 1$ or 0 . To simplify statement, we denote $p_{ij} = \mathbb{P}(Y^* = j | Y = i)$ for $i, j = 1$ or 0 , where p_{01} is the false positive rate of the disease and p_{10} is the false negative rate of the disease. Let $v = \mathbb{P}(Y = 1)$ denote the disease prevalence in the target population. Since v , p_{01} , and p_{10} are usually attainable through existing literature and medical expert consultations, we assume these values are known.

Let $s = \mathbb{P}(S = 1 | Y^* = 0) / \mathbb{P}(S = 1 | Y^* = 1)$ denote the sampling ratio between cases and controls. This ratio measures the degree of sampling bias, with $s = 1$ indicating random sampling, and as s deviates further from 1, the level of selection bias increases. Let $v^* = \mathbb{P}(Y^* = 1)$ denote the observed disease prevalence, which may differ from v due to measurement error. Let $g_i^*(x) = \mathbb{E}[Y^* | X = x, T = i, S = 1]$ denote the expectation of Y^* conditional on $X = x$, $T = t$, and $S = 1$, which can be identified by the sample distribution. The following lemma explores the relationship between $g_i^*(x)$ and $g_i(x)$.

LEMMA 2.1: *Under Assumptions 1-5, for $i = 0$ or 1 , we have*

$$g_i^*(X) = \frac{((1 - p_{10} - p_{01})g_i(X) + p_{01})s}{1 + ((1 - p_{10} - p_{01})g_i(X) + p_{01})(s - 1)}, \quad (2)$$

where

$$s = \frac{\mathbb{P}(Y^* = 1 | S = 1) / v^*}{\mathbb{P}(Y^* = 0 | S = 1) / (1 - v^*)}, \quad (3)$$

$$v^* = (1 - p_{10} - p_{01})v + p_{01}. \quad (4)$$

Lemma 2.1 indicates that the sampling ratio s and observed disease prevalence v^* are determined by v , p_{01} and p_{10} . Also, there is a one-to-one function relationship between $g_i^*(X)$ and $g_i(X)$ given v , p_{01} and p_{10} , which demonstrates that $g_i(X)$ is identifiable since $g_i^*(X)$ is determined by the sample distribution. To ensure the identifiability of τ , one must also calculate the expectation of $g_i(X)$.

LEMMA 2.2: Under Assumptions 1-5, for $i = 0$ or 1 , we have

$$\mathbb{E}[g_i(X)] = v^*u_{i1} + (1 - v^*)u_{i0}, \quad (5)$$

where

$$u_{ij} = \int g_i(x)f(x|Y^* = j, S = 1)dx, \quad (6)$$

v^* is given in (4) and $f(\cdot | Y^*, S)$ represents the conditional density of X given Y^* and S .

The proof of Lemma 2.2 is straightforward by applying the law of total probability and Assumption 4. Applying Lemmas 2.1-2.2, we can establish the identifiability of τ , as described in Theorem 2.1.

THEOREM 2.1: Under Assumptions 1-5, the average treatment effect τ is identifiable:

$$\tau = \mathbb{E}[g_1(X)] - \mathbb{E}[g_0(X)],$$

where

$$\begin{aligned} \mathbb{E}[g_i(X)] = & \frac{v^*}{1 - p_{10} - p_{01}} \int \left(\frac{g_i^*(x)}{s - g_i^*(x)(s - 1)} - p_{01} \right) f(x|Y^* = j, S = 1)dx \\ & + \frac{1 - v^*}{1 - p_{10} - p_{01}} \int \left(\frac{g_i^*(x)}{s - g_i^*(x)(s - 1)} - p_{01} \right) f(x|Y^* = j, S = 1)dx, \quad i = 1, 0, \quad (7) \end{aligned}$$

where s and v^* are given in (3) and (4), respectively.

Since $\mathbb{P}(Y^*, X, T|S = 1)$ can be approximated by its sample version, we can consistently estimate ATE τ if p_{01}, p_{10}, v are given. We provide methods for estimating τ in the next section.

3. Estimation of ATE τ

In this section, we derive the estimation bias of naive method ignoring selection sampling and mismeasurement, then propose two debias methods. Both methods depend on an adjusted link function associated with sampling ratio s and mismeasurement probabilities p_{01} and p_{10} .

According to Theorem 2.1, to estimate τ , we can first estimate g_i then estimate $\mathbb{E}[g_i(X)]$,

$i = 0, 1$. To begin with, we model g_i with a logistic link:

$$g_i(x) = \frac{\exp(\eta(T = i, X = x))}{1 + \exp(\eta(T = i, X = x))},$$

where the index $\eta(t, x)$ is a function of t and x . Applying Lemma 2.1, we obtain that

$$g_i^*(x) = h(\eta(T = i, X = x)),$$

where

$$h(\eta) = \frac{(p_{01} + \exp(\eta)(1 - p_{10}))s}{1 + p_{01}(s - 1) + \exp(\eta)(1 + (1 - p_{10})(s - 1))}. \quad (8)$$

serves as an adjusted link function. The log-likelihood function of the observed samples is

$$\ell_n(y^*, \eta(t, \mathbf{x})) = \sum_{i=1}^n \left\{ y_i^* \log\left(\frac{\mu_i}{1 - \mu_i}\right) + \log(1 - \mu_i) \right\}, \quad (9)$$

where $\mu_i = h(\eta(t_i, \mathbf{x}_i))$ for i -th sample and n is the size of sample.

Remark 1: The adjusted link function $h(\eta)$ is a monotone increasing function of index η . The shape of its curve is highly influenced by the values of p_{01} , p_{10} , and s . For example, the function has a supremum of $\frac{(1-p_{10})s}{1+(1-p_{10})(s-1)}$ and an infimum of $\frac{p_{01}s}{1+p_{01}(s-1)}$. Figure 4 in Appendix B of Supplementary Materials illustrates the curves of $h(\eta)$ for various combinations of p_{01} , p_{10} , and s . It is worth noting that when $p_{01} = 0$, $p_{10} = 0$, and $s = 1$, $h(\eta)$ degenerate to the logistic link function, corresponding to the situation of random sampling and no measurement error.

Remark 2: As shown in Figure 4, when $p_{01} > 0$, $p_{10} > 0$, and $s > 1$, the shape of the curves becomes deflated and shifted. Especially when s is large and p_{01} is bigger than 0, the infimum of $h(\eta)$ approaches 1. This leads to a significantly reduced range of the adjusted link function, which in turn makes model estimation challenging. To avoid an excessively small range of $h(\eta)$ when s is big, it is crucial to ensure that p_{01} does not deviate too far from 0. Fortunately, in real world, p_{01} is often very close to 0, maintaining a reasonable range for the η function.

Remark 3: Consider the ODS design with no measurement error, that is $p_{01} = 0$, $p_{10} = 0$ and $s > 1$. If we further assume that η has a linear form $\eta(t, \mathbf{x}) = a_0 + a_1T + \mathbf{b}^\top \mathbf{x}$, then the

logistic regression produces consistent estimates of the slope parameters a_1 and \mathbf{b}^\top . However, when it comes to ODS design with measurement error, that is $p_{01} > 0$, $p_{10} > 0$ and $s > 1$, all the logistic regression estimators will be biased. Details can be seen in Czado and Santner (1992).

3.1 A generalized linear model based estimator

In this subsection, we assume that the true model for $\eta(t, \mathbf{x})$ has a linear form: $\eta(t, \mathbf{x}) = a_0 + a_1 T + \mathbf{b}^\top \mathbf{x}$. Denote $\boldsymbol{\beta}^\top = (a_0, a_1, \mathbf{b}^\top)$. The estimation of $\boldsymbol{\beta}$ can be performed by maximizing the log-likelihood function of GLM with the adjusted link function $h(\cdot)$. The estimation of τ can then be obtained by following the subsequent steps.

Step 0: Determine the values of p_{10}, p_{01}, v .

Step 1: Estimate sampling ratio s and the adjusted link function h . Motivated by (3), we obtain an estimator of s by solving the estimating equation.

$$S_n(s) := \frac{1}{n} \sum_{i=1}^n \{s v^* (1 - y_i^*) - (1 - v^*) y_i^*\} = 0. \quad (10)$$

Denote the resulting estimator by $\hat{s} = \frac{\sum_{i=1}^n y_i^* (1 - v^*)}{\sum_{i=1}^n (1 - y_i^*) v^*}$. Plugging \hat{s} in (8), we obtain an estimator of the link function $h(\cdot)$, denoted as $\hat{h}(\cdot)$.

Step 2: Estimate $\boldsymbol{\beta}$. We can estimate $\boldsymbol{\beta}$ by solving the following score equations:

$$G_n(\boldsymbol{\beta}) := \frac{1}{n} \frac{\partial \ell_n(\boldsymbol{\beta})}{\partial \boldsymbol{\beta}} = 0, \quad (11)$$

where $\ell_n(\boldsymbol{\beta})$ is defined in (9), with $h(\cdot)$ being replaced by $\hat{h}(\cdot)$. Denote the resulting estimator by $\hat{\boldsymbol{\beta}}^\top = (\hat{a}_0, \hat{a}_1, \hat{\mathbf{b}}^\top)$. Denote $\hat{g}_1(x) = \text{expit}(\hat{a}_0 + \hat{a}_1 + \hat{\mathbf{b}}^\top x)$ and $\hat{g}_0(x) = \text{expit}(\hat{a}_0 + \hat{\mathbf{b}}^\top x)$.

Step 3: Estimate $\mathbf{u} = (u_{11}, u_{10}, u_{01}, u_{00})^\top$. Inspired by (6), we can get the estimators of u_{ij} by

$$\begin{aligned} \hat{u}_{11} &= \frac{1}{\sum_{i=1}^n y_i^*} \sum_{i=1}^n y_i^* \hat{g}_1(x_i), & \hat{u}_{10} &= \frac{1}{\sum_{i=1}^n (1 - y_i^*)} \sum_{i=1}^n (1 - y_i^*) \hat{g}_1(x_i), \\ \hat{u}_{01} &= \frac{1}{\sum_{i=1}^n y_i^*} \sum_{i=1}^n y_i^* \hat{g}_0(x_i), & \hat{u}_{00} &= \frac{1}{\sum_{i=1}^n (1 - y_i^*)} \sum_{i=1}^n (1 - y_i^*) \hat{g}_0(x_i). \end{aligned}$$

Step 4: Estimate the average treatment effect τ . According to (5), we can estimate τ by

$$\hat{\tau} = [v^* \hat{u}_{11} + (1 - v^*) \hat{u}_{10}] - [v^* \hat{u}_{01} + (1 - v^*) \hat{u}_{00}],$$

where v^* is calculated according to (4).

To establish the asymptotic distribution of estimated parameters, we write steps 1-3 in a form of estimation equations:

$$\begin{pmatrix} S_n(s) \\ G_n(s, \boldsymbol{\beta}) \\ M_n(\boldsymbol{\beta}, \mathbf{u}) \end{pmatrix} =: \frac{1}{n} \sum_i^n \boldsymbol{\psi}(y_i^*, x_i, t_i, \boldsymbol{\theta}) = 0, \quad (12)$$

where $\boldsymbol{\theta}^\top = (s, \boldsymbol{\beta}^\top, \mathbf{u}^\top)$, $\mathbf{u}^\top = (u_{11}, u_{10}, u_{01}, u_{11})$ and

$$M_n(\mathbf{u}, \boldsymbol{\beta}) := \frac{1}{n} \sum_{i=1}^n \begin{pmatrix} y_i^*(u_{11} - g_1(x_i, \boldsymbol{\beta})) \\ (1 - y_i^*)(u_{10} - g_1(x_i, \boldsymbol{\beta})) \\ y_i^*(u_{01} - g_0(x_i, \boldsymbol{\beta})) \\ (1 - y_i^*)(u_{00} - g_0(x_i, \boldsymbol{\beta})) \end{pmatrix}.$$

Denoting the resulting estimator by $\hat{\boldsymbol{\theta}} = (\hat{s}, \hat{\boldsymbol{\beta}}^\top, \hat{\mathbf{u}}^\top)^\top$, we have the following theorem.

THEOREM 3.1: Let $\boldsymbol{\theta}_0$ denote the true parameter values for $\boldsymbol{\theta}$. If the true index function η has the linear form $\eta(t, \mathbf{x}) = a_0 + a_1 t + \mathbf{b}^\top \mathbf{x}$, then under some regularity conditions given in Appendix A of Supplementary Materials, we have that $\hat{\boldsymbol{\theta}}$ is consistent for $\boldsymbol{\theta}_0$, and

$$\sqrt{n}(\hat{\boldsymbol{\theta}} - \boldsymbol{\theta}_0) \xrightarrow{d} N(0, \mathbf{V}(\boldsymbol{\theta}_0)),$$

where the limiting variance of $\sqrt{n}\hat{\boldsymbol{\theta}}$ can be written as the sandwich matrix form: $\mathbf{V}(\boldsymbol{\theta}_0) = \mathbf{H}(\boldsymbol{\theta}_0)^{-1} \mathbf{B} \{ \mathbf{H}(\boldsymbol{\theta}_0)^{-1} \}^\top$ with $\mathbf{B}(\boldsymbol{\theta}_0) = \mathbb{E} \{ \boldsymbol{\psi}(Y^*, X, T, \boldsymbol{\theta}_0) \boldsymbol{\psi}(Y^*, X, T, \boldsymbol{\theta}_0)^\top | S = 1 \}$ and $\mathbf{H}(\boldsymbol{\theta}_0) = \mathbb{E} \{ \partial \boldsymbol{\psi}(Y^*, X, T, \boldsymbol{\theta}_0) / \partial \boldsymbol{\theta}_0^\top | S = 1 \}$.

Utilizing Theorem 3.1, we can estimate τ by $\hat{\tau}_{\text{GLM}} = \mathbf{q}^\top \hat{\boldsymbol{\theta}}$, where $\mathbf{q}^\top = (\mathbf{0}^\top, \mathbf{c}^\top)$, $\mathbf{c}^\top = (v^*, v^* - 1, v^*, v^* - 1)$. Subsequently, applying the Slutsky Theorem, we obtain the asymptotic

normality of $\hat{\tau}_{\text{GLM}}$:

$$\sqrt{n}(\hat{\tau}_{\text{GLM}} - \tau) \xrightarrow{d} N(0, \mathbf{q}^\top \mathbf{V}(\boldsymbol{\theta}_0) \mathbf{q}).$$

The covariance matrix $\mathbf{V}(\boldsymbol{\theta}_0)$ can be estimated by $\hat{\mathbf{V}}(\boldsymbol{\theta}_0) = \hat{\mathbf{H}}^{-1} \hat{\mathbf{B}} \{ \hat{\mathbf{H}}^{-1} \}^\top$, where $\hat{\mathbf{H}} = -\frac{1}{n} \sum_{i=1}^n \boldsymbol{\psi}'(y_i^*, x_i, t_i, \hat{\boldsymbol{\theta}})$ and $\hat{\mathbf{B}} = \frac{1}{n} \sum_{i=1}^n \boldsymbol{\psi}(y_i^*, x_i, t_i, \hat{\boldsymbol{\theta}}) \boldsymbol{\psi}(y_i^*, x_i, t_i, \hat{\boldsymbol{\theta}})^\top$. This allows us to make statistical inference regarding τ .

3.2 A generalized additive model based estimator

In real-world studies, the linearity assumption of $\eta(t, \mathbf{x})$ is often violated. To enhance the robustness of our method, we employ the generalized additive model (Hastie and Tibshirani, 1987; Marx and Eilers, 1998) to capture the nonlinear characteristics of $\eta(t, \mathbf{x})$. This approach enables us to develop an improved estimator that is resilient to model misspecification.

To begin with, we denote by $\tilde{\eta}(t_i, \mathbf{x}_i)$ the true index of the i -th individual and $\eta(t_i, \mathbf{x}_i)$ a working index. We assume $\tilde{\eta}(t_i, \mathbf{x}_i)$ has the following additive form:

$$\tilde{\eta}(t_i, \mathbf{x}_i) = at_i + \sum_{j=1}^D \tilde{\eta}_j(x_{ij}), \quad j = 1, \dots, D, \quad (13)$$

where x_{ij} is the j -th covariate of i -th sample. We also assume that $\mathbb{E}[\tilde{\eta}_j(X_{ij})] = 0$ for $j = 1, \dots, D$ to ensure the identifiability of $\tilde{\eta}_j$. We approximate $\tilde{\eta}_j(x_{ij})$ by the following B-spline model:

$$\eta_j(x_{ij}) = \sum_{k=-p+1}^{K_n} B_k^p(x_{ij}) b_{k,j}, \quad j = 1, \dots, D,$$

where $B_k^p(x)$ is the p -th B-spline functions defined recursively ($k = -p + 1, \dots, K_n$) (De Boor, 1978). Here K_n is the number of knots, p is the degree of B-spline, and $b_{k,j}$'s are unknown parameters. To simplify notation, we denote $B_k^p(x)$ as $B_k(x)$, unless we explicitly state the degree of the B-spline. Our primary focus henceforth will be on the p -th B-spline. We model the index of the i -th sample as

$$\eta(t_i, \mathbf{x}_i) = at_i + \sum_{j=1}^D \sum_{k=-p+1}^{K_n} B_k(x_{ij}) b_{k,j} = at_i + \sum_{j=1}^D \mathbf{B}(x_{ij})^\top \mathbf{b}_j = \mathbf{Z}_i \boldsymbol{\beta},$$

where $\mathbf{Z}_i = (\mathbf{B}(x_{i1})^\top, \dots, \mathbf{B}(x_{iD})^\top, t_i)$, $\mathbf{B}(x) = (B_{-p+1}(x), \dots, B_{K_n}(x))^\top$, $\boldsymbol{\beta}^\top = (\mathbf{b}^\top, a)$,

$\mathbf{b}^\top = (\mathbf{b}_1^\top, \dots, \mathbf{b}_D^\top)$, and $\mathbf{b}_j = \{b_{k,j}\}_{k=-p+1}^{K_n}$, $j = 1, \dots, D$. Note that the dimension of $\boldsymbol{\beta}$ is $D(K_n + p) + 1$.

The observed log-likelihood function based on the above B-spline approximation shares the same form as (9), except that η is no longer the true index function $\tilde{\eta}$. We then utilize the ridge-corrected penalized log-likelihood function proposed by Marx and Eilers (1998) and Yoshida and Naito (2014):

$$\ell_{\text{rp},n}(\boldsymbol{\beta}, \lambda_n, \gamma_n) = \ell_n(\boldsymbol{\beta}) - \sum_{j=1}^D \frac{\lambda_{jn}}{2n} \mathbf{b}_j^\top \Delta_m^\top \Delta_m \mathbf{b}_j - \frac{\gamma_n}{2n} \sum_{j=1}^D \mathbf{b}_j^\top \mathbf{b}_j, \quad (14)$$

where $\lambda_n = \{\lambda_{jn}\}_{j=1}^D$ and γ_n are tuning parameters. Δ_m is the m -th order difference matrix (Dierckx, 1995). The spline parameters are subject to penalization, where the first penalty term is a usual trick in the penalized spline estimators to prevent the estimate from wriggling when the spline dimension $D(K_n + p)$ is large, and the second penalty term aims to ensure the nonsingularity of the Hessian matrix of $\ell_{\text{rp},n}(\boldsymbol{\beta}, \lambda_n, \gamma_n)$. The score functions are obtained with

$$G_{\text{rp},n}(\boldsymbol{\beta}, \lambda_n, \gamma_n) = \frac{\partial \ell_{\text{rp},n}(\boldsymbol{\beta}, \lambda_n, \gamma_n)}{\partial \boldsymbol{\beta}}. \quad (15)$$

Similar to the operations in Section 3.1, we can obtain an estimator of τ by applying Steps 0-4 with G_n in Step 2 being replaced by $G_{\text{rp},n}$. Also, we write Steps 1-3 in a form of estimating equations:

$$\begin{pmatrix} S_n(s) \\ G_{\text{rp},n}(\boldsymbol{\beta}, s, \lambda_n, \gamma_n) \\ M_n(\mathbf{u}, \boldsymbol{\beta}) \end{pmatrix} =: \frac{1}{n} \sum_{i=1}^n \boldsymbol{\psi}(y_i^*, x_i, t_i, \boldsymbol{\theta}, \lambda_n, \gamma_n) = 0. \quad (16)$$

Denote the resulting estimators as $\hat{\boldsymbol{\theta}} = (\hat{s}, \hat{\boldsymbol{\beta}}^\top, \hat{\mathbf{u}}^\top)^\top$. Note that, unlike (12), the dimension of $\boldsymbol{\psi}$ in (16) is not fixed, which increases with the sample size n . Similarly, The ATE τ can be estimated by $\hat{\tau}_{\text{GAM}} = \mathbf{q}^\top \hat{\boldsymbol{\theta}}$.

Before stating asymptotic properties of $\hat{\tau}_{\text{GAM}}$, we introduce some notations. Let $\boldsymbol{\theta}_0 =$

$(s_0, \boldsymbol{\beta}_0^\top, \mathbf{u}_0^\top)^\top$, where s_0 is the solution of $\mathbb{E}[S_n(s)|S=1]=0$, $\boldsymbol{\beta}_0 = \underset{\boldsymbol{\beta}}{\operatorname{argmin}} \mathbb{E} \left[\log \frac{f(Y, \mathbf{X}, \tilde{\eta})}{f(Y, \mathbf{X}, \boldsymbol{\beta})} | S=1 \right]$ is the best spline approximation of the true index function $\tilde{\eta}(t, \mathbf{x})$ based on Kullback-Leibler measure and \mathbf{u}_0 is the solution of $\mathbb{E}[M_n(\mathbf{u}, \boldsymbol{\beta}_0)|S=1]=0$. Let τ denote the true value of ATE. We have the following asymptotic results for τ_{GAM} .

THEOREM 3.2: *If the true index function $\tilde{\eta}$ obeys the additive form as (13), then under some regularity conditions in Appendix A of Supplementary Materials, we have that $\hat{\tau}_{\text{GAM}}$ is consistent for τ , and $\hat{\tau}_{\text{GAM}} - \tau$ is asymptotically normal with asymptotic mean $\mathbf{Bias}(\hat{\tau}_{\text{GAM}})$ (refer to (A.14) in Appendix A for an explicit expression), and asymptotic covariance $\mathbf{V}(\hat{\tau}_{\text{GAM}}) = \frac{1}{n} \mathbf{q}^\top \tilde{\mathbf{H}}(\lambda_n)^{-1} \tilde{\mathbf{B}} \{ \tilde{\mathbf{H}}(\lambda_n)^{-1} \}^\top \mathbf{q}$, where*

$$\tilde{\mathbf{H}}(\lambda_n) = \mathbb{E} \left\{ \tilde{\boldsymbol{\psi}}'(Y^*, X, T, \boldsymbol{\theta}_0, \lambda_n, \gamma_n = 0) | S = 1 \right\},$$

$$\tilde{\mathbf{B}} = \mathbb{E} \left\{ \tilde{\boldsymbol{\psi}}(Y^*, X, T, \boldsymbol{\theta}_0, \lambda_n = 0, \gamma_n = 0) \tilde{\boldsymbol{\psi}}(Y^*, X, T, \boldsymbol{\theta}_0, \lambda_n = 0, \gamma_n = 0)^\top | S = 1 \right\}.$$

Refer to (A.5) and (A.6) in Appendix A for explicit expressions of $\tilde{\boldsymbol{\psi}}$ and $\tilde{\boldsymbol{\psi}}'$, respectively. Furthermore, $\mathbf{Bias}(\hat{\tau}_{\text{GAM}}) = O(n^{-(p+1)/(2p+3)})$ and $\mathbf{V}(\hat{\tau}_{\text{GAM}}) = O(n^{-2(p+1)/(2p+3)})$.

Remark 1: Theorem 3.2 demonstrates that $\hat{\tau}_{\text{GAM}}$ is $n^{-(p+1)/(2p+3)}$ -consistent and asymptotic normal, and the asymptotic order of $\hat{\tau}_{\text{GAM}}$'s mean squared error is $O(n^{-2(p+1)/(2p+3)})$. These results coincide with those of Yoshida and Naito (2014).

Remark 2: If the true index follows a linear form, then $\hat{\tau}_{\text{GLM}}$ proposed in Section 3.1 is $n^{-1/2}$ -consistent. However, $\hat{\tau}_{\text{GLM}}$ is generally sensitive to the linear assumption. On the other hand, $\hat{\tau}_{\text{GAM}}$ has a much wider applicability, subject to a lower efficiency in terms of convergence rate.

Remark 3: In large sample cases, $\mathbf{V}(\hat{\tau}_{\text{GAM}})$ can be consistently approximated by $\hat{\mathbf{V}}(\hat{\tau}_{\text{GAM}}) = \frac{1}{n} \mathbf{q}^\top \hat{\mathbf{H}}^{-1} \hat{\mathbf{B}} \{ \hat{\mathbf{H}}^{-1} \}^\top \mathbf{q}$, with $\hat{\mathbf{H}} = -\frac{1}{n} \sum_{i=1}^n \boldsymbol{\psi}'(y_i^*, x_i, t_i, \hat{\boldsymbol{\theta}}, \lambda_n, \gamma_n = 0)$ and $\hat{\mathbf{B}} = \frac{1}{n} \sum_{i=1}^n \boldsymbol{\psi}(y_i^*, x_i, t_i, \hat{\boldsymbol{\theta}}, \lambda_n = 0, \gamma_n = 0) \boldsymbol{\psi}(y_i^*, x_i, t_i, \hat{\boldsymbol{\theta}}, \lambda_n = 0, \gamma_n = 0)^\top$. Statistical inference of τ can be made according to the asymptotic normality of $\hat{\tau}_{\text{GAM}}$.

4. Simulation studies

In this section, we evaluate the finite-sample performance of our proposed GLM-EE and GAM-EE methods through simulations.

4.1 Data generation

The data generation process consists of two steps: data pool creation and case-control sample selection. We start by creating a data pool representing the target population, where each patient's true disease status and diagnosis status are generated. We independently sample two continuous covariates, X_1 and X_2 , from a standard normal and uniform distribution, respectively. Another discrete covariate, U , is sampled from a Bernoulli distribution with $\mathbb{P}(U = 1) = 0.5$. The treatment indicator T is sampled from a Bernoulli distribution with $\mathbb{P}(T = 1|X_1, X_2, U) = \text{expit}(1 + 0.1X_1 - 0.1X_2 - 0.5U)$. To demonstrate the utility of our methods in both linear and nonlinear settings, we consider the following outcome models:

$$\mathbf{M1:} \quad \tilde{\eta} = a_0 - 2T - U - 0.5X_1 + X_2;$$

$$\mathbf{M2:} \quad \tilde{\eta} = a_0 - 2T - U - \sin(3\pi X_1) + (3(X_2 - 0.5))^3;$$

$$\mathbf{M3:} \quad \tilde{\eta} = a_0 - 2T - U - \exp(2X_1) - \sin(3\pi X_2)X_2;$$

$$\mathbf{M4:} \quad \tilde{\eta} = a_0 - 2T - U - \exp(2X_1) + (3(X_2 - 0.5))^3 + X_1X_2.$$

M1 is a typical linear model. **M2-M3** are non-linear but still follows the additive form in (13). **M4** violates both linear and additive assumptions. In all the models, the intercept term a_0 is set based on a predetermined disease prevalence v . The true outcome Y is sampled from the Bernoulli distribution with success probability $\text{expit}(\tilde{\eta})$. We then generate the observed outcome Y^* based on Y with conditional probability p_{10} and p_{01} . Thus we construct a data pool to simulate a population of size 1000,000. We then randomly sample $n/2$ cases and $n/2$ controls from the data pool based on the observed outcome Y^* 's, but with only Y^*, T, U, X_1, X_2 kept in the subsequent analysis.

We fix $p_{01} = 0$ as it is usually very small in practice. We consider various combinations of

v , p_{10} , and n . That is, $v = 0.001, 0.01, \text{ and } 0.1$, $p_{01} = 0, 0.2, \text{ and } 0.4$, $n = 500 \text{ and } 2000$. For each combination of v and outcome model, the true τ are calculated through Monte Carlo integration. When applying the GAM-EE method, the number of knots for X_1 and X_2 is set to be $K_n = 10$, and the value of λ_n is selected based on the Bayesian information criterion as in Marx and Eilers (1998), and γ_n is set to be 0.1. For each combination of v , p_{10} , p_{01} , n , and outcome model, we repeat simulations for 500 times.

4.2 *Debias capacity of GLM-EE and GAM-EE*

We first evaluate the debiasing capability of our proposed methods in model **M1**, where the true index has a linear form. Along with the standard GLM-EE and GAM-EE methods, we also consider three naive estimators based on the GLM-EE method and three naive estimators based on the GAM-EE method. These naive estimators are obtained by applying the GLM-EE and GAM-EE methods but intentionally ignoring the information of measurement and selection (i.e., manually fix $p_{10} = 0$ and $s = 1$ when applying the GLM-EE and GAM-EE methods). The EE methods ignoring measurement information, selection information, and both information are denoted as “naive 3”, “naive 2” and “naive 1”, respectively. We also consider the IPTW method as a comparison.

Figure 2 depicts the box plots of the ATE estimators. The standard GLM-EE and GAM-EE estimators’ box covers the true τ (represented by the red line), and the empirical means closely align with the true τ . Conversely, the naive and IPTW estimators exhibit obvious bias, as their boxes fail to cover the true τ . The biases are particularly large for IPTW, naive 1, and naive 2, and they are much bigger than naive 3. This observation suggests that the biases are primarily due to sampling bias instead of measurement error.

To further compare the performance of standard GAM-EE and GLM-EE methods, we present the relative biases, root mean squared errors, coverage probabilities of $\hat{\tau}_{\text{GLM}}$ and $\hat{\tau}_{\text{GAM}}$ in Table 1. Both $\hat{\tau}_{\text{GLM}}$ and $\hat{\tau}_{\text{GAM}}$ produce fairly small empirical biases and reasonable

coverage probabilities close to the nominal level of 95%. Furthermore, $\hat{\tau}_{\text{GAM}}$ has slightly bigger RMSEs than $\hat{\tau}_{\text{GLM}}$ since GAM-EE requires to estimate more parameters than GLM-EE.

[Figure 2 about here.]

[Table 1 about here.]

4.3 Robustness of GLM-EE and GAM-EE

To evaluate the robustness of our methods, we conduct a detailed comparison between the standard GLM-EE method ($\hat{\tau}_{\text{GLM}}$) and the standard GAM-EE method ($\hat{\tau}_{\text{GAM}}$) in different nonlinear model settings. Tables 2 summarize the results of model **M2** and **M3**, where the GLM-EE method suffers from the problem of model misspecification. In the simulation situations, $\hat{\tau}_{\text{GLM}}$ produces systematic biases, depending on the prevalence v (the lower the prevalence, the larger the bias). On the other hand, $\hat{\tau}_{\text{GAM}}$ produces consistently smaller empirical biases and RMSEs than $\hat{\tau}_{\text{GLM}}$, especially in model **M3**. The coverage probabilities of $\hat{\tau}_{\text{GAM}}$ are also close to the nominal level of 95%. This demonstrates the high performance of the GAM-EE method in nonlinear but additive settings. Table 3 shows the results for model **M4**, where both GLM-EE and GAM-EE methods suffer from model misspecification problems, but $\hat{\tau}_{\text{GAM}}$ has smaller biases and RMSEs in general.

[Table 2 about here.]

[Table 3 about here.]

Overall, The GAM-EE method outperforms the GLM-EE method in nonlinear settings and loses little statistical efficiency compared with the GLM-EE method in linear settings. The above results support the theoretical results established in Section 3. For scenarios where $p_{01} > 0$, as discussed in Section 3, the estimate of τ is not stable if v is rather small. We increase the sample sizes to $n = 3000$ and only consider four combinations of p_{01} and v (i.e,

$p_{01} = 0.03, 0.06,$ and $v = 0.05, 0.1$). Tables 4 in Appendix B of Supplementary Materials summarize the corresponding results, showing the same behaviors as scenarios with $p_{01} = 0$.

5. Real data analysis

In this section, we apply the GAM-EE and GLM-EE methods to a real-world example. We aim to analyze the effect of alcohol intake on the risk of developing gout. We use data from the UK BioBank database, a large-scale prospective cohort study including 502,543 volunteer participants aged 37 to 73 years from UK between 2007 and 2010. We collected information on the treatment (alcohol intake), the observed outcome (gout diagnosis status), and covariates including education level, ethnicity, diet score (summarized score of diet habits), BMI, physical exercise, TDI (Townsend deprivation index), age, and household income. After eliminating the missing data and limiting our sample to only males, we obtained a target population of 136,741 subjects (refer to Table 6 in Appendix B of Supplementary Materials for detailed information). Within this population, 3.85% subjects are diagnosed with gout ($v^* = 3.85\%$), but the true disease prevalence v is unknown. However, if we know the values of false positive rate p_{01} and false negative rate p_{10} , we can calculate the true disease prevalence by $v = (v^* - p_{01}) / (1 - p_{10} - p_{01})$ according to (4). We apply our proposed GLM-EE and GAM-EE methods to the dataset. When applying the GAM-EE method, the number of knots K_n is fixed to be 5. The value of λ_n is selected based on the Bayesian information criterion from a candidate sequence ranging from 1 to 20, and γ_n is set to be 0.1.

First, we aim to extend the discussion in Section 4 with the purpose of evaluating the validity of our proposed EE methods, leveraging the full dataset. The corresponding results can be regarded as benchmarks. It is important to mention that while the full dataset does not have the bias sampling problem, it still suffers from measurement error problems. We draw a case-control subsample from the full dataset based on the diagnosed status, with the same case and control size of 2500. The subsample suffers from both selection and

mismeasurement biases. We then apply GAM-EE and GLM-EE methods to the subsample. This process is repeated for 500 times. Figure 5 in Appendix B of Supplementary Materials depicts the box plots of our estimators. The results given by GAM-EE method are fairly close to the corresponding benchmarks, with differences ranging from 1×10^{-7} to 1×10^{-2} . On the other hand, the results given by GLM-EE method deviate from the corresponding benchmark, with differences ranging from 1×10^{-6} to 2×10^{-2} . The standard errors of the two methods are close to each other. These results indicate that GAM-EE method is more robust than GLM-EE method in this example.

Second, we demonstrate the practical utility of our methods in real-world research by conducting a sensitivity analysis. This time we only have a case-control subsample and the real disease status is unobserved. Based on literature review (Vázquez-Mellado et al., 2012; Kiefer et al., 2016) and experts experience, we determine possible ranges of disease prevalence $v \in (0.030, 0.045)$, false positive rate $p_{10} \in (10\%, 30\%)$, and false negative rate $p_{01} \in (0\%, 6\%)$. We select several breakpoints within these ranges, apply our methods, and summarize the results in Figure 3. Evidently, within the possible ranges of v , p_{10} , and p_{01} , the estimated τ is significantly greater than 0, in terms of 95% confidence intervals. The median ATE ranges from 0.01 to 0.04, depending on the specification of v , p_{01} and p_{10} . Therefore, we conclude that alcohol intake has a significant positive ATE on the risk of developing gout.

[Figure 3 about here.]

6. Discussion

This paper presents novel methods for addressing an analytical challenge that arises when conducting causal inference in the context of outcome-dependent sampling (ODS) design with measurement error. In such scenarios, ordinary ATE estimators are susceptible to selection and mismeasurement biases. Our proposed GLM-EE and GAM-EE methods leverage

additional information from the target population on disease prevalence and mismeasurement rates to address the biases. The effectiveness of our methods for eliminating the influence of ODS and mismeasurement appears to be robust to the specification of outcome models in simulation studies. We also provide practical guidance for conducting sensitivity analysis in real-world ODS studies. We apply our methods to the UK Biobank dataset to estimate ATE of alcohol intake on gout. Our methods demonstrated promising performance in this application.

Our methods focus on estimating ATE, although they can readily be extended to estimate other causal effect measures of interest, such as the causal risk ratio and the causal odds ratio. Furthermore, although we consider a scenario with two treatment options, our methods can be generalized to multiple treatment arms.

As discussed in Section 3, the adjusted link function may be quite flat in cases where v is small and $p_{01} > 0$. This can lead to instability in solving the estimating equations, necessitating a large sample size to ensure convergence. However, The increase in sample size will highly increase the computation time, especially when the dimension of covariates or the size of the knots is big. As a result, when $p_{01} > 0$, we only consider scenarios where the disease prevalence v is not small. This limitation may restrict the generalizability of our methods and we leave this interesting topic as a future work to explore.

Overall, our proposed methods provide a valuable tool for addressing the analytical challenges associated with causal inference in the presence of ODS and measurement error. Our methods offer a practical and effective means in obtaining unbiased estimates of ATE, even when the outcome model is not linear.

ACKNOWLEDGEMENTS

The work of HZ is partly supported by the National Natural Science Foundation of China (7209121, 12171451). This research has been conducted using the UK Biobank resource (application number 96744), subject to a data transfer agreement.

DADA AVAILABILITY STATEMENT

The data that support the findings in this paper can be obtained from the UK Biobank (<http://www.ukbiobank.ac.uk>).

SUPPLEMENTARY MATERIALS

Appendix A (referenced in Section 2-3) and Appendix B (referenced in Sections 3-5) are available.

REFERENCES

- Angrist, J. D., Imbens, G. W., and Rubin, D. B. (1996). Identification of causal effects using instrumental variables. *Journal of the American Statistical Association* **91**, 444–455.
- Angrist, J. D. and Krueger, A. B. (2001). Instrumental variables and the search for identification: From supply and demand to natural experiments. *Journal of Economic Perspectives* **15**, 69–85.
- Bareinboim, E. and Pearl, J. (2016). Causal inference and the data-fusion problem. *Proceedings of the National Academy of Sciences* **113**, 7345–7352.
- Barrow, D. and Smith, P. (1978). Asymptotic properties of best $l_2[0, 1]$ approximation by splines with variable knots. *Quarterly of Applied Mathematics* **36**, 293–304.
- Beesley, L. J. and Mukherjee, B. (2022). Statistical inference for association studies using electronic health records: handling both selection bias and outcome misclassification. *Biometrics* **78**, 214–226.

- Breslow, N. E. and Holubkov, R. (1997). Maximum likelihood estimation of logistic regression parameters under two-phase, outcome-dependent sampling. *Journal of the Royal Statistical Society: Series B (Statistical Methodology)* **59**, 447–461.
- Copeland, K. T., Checkoway, H., McMichael, A. J., and Holbrook, R. H. (1977). Bias due to misclassification in the estimation of relative risk. *American Journal of Epidemiology* **105**, 488–495.
- Czado, C. and Santner, T. J. (1992). The effect of link misspecification on binary regression inference. *Journal of Statistical Planning and Inference* **33**, 213–231.
- De Boor, C. (1978). *A Practical Guide to Splines*, volume 27. Springer, New York.
- Dierckx, P. (1995). *Curve and Surface Fitting With Splines*. Oxford University Press, Oxford.
- Fox, M. P., Lash, T. L., and Greenland, S. (2005). A method to automate probabilistic sensitivity analyses of misclassified binary variables. *International Journal of Epidemiology* **34**, 1370–1376.
- Fox, M. P., MacLehose, R. F., and Lash, T. L. (2022). *Applying Quantitative Bias Analysis to Epidemiologic Data*. Springer, New York.
- Gabriel, E. E., Sachs, M. C., and Sjölander, A. (2022). Causal bounds for outcome-dependent sampling in observational studies. *Journal of the American Statistical Association* **117**, 939–950.
- Hastie, T. and Tibshirani, R. (1987). Generalized additive models: Some applications. *Journal of the American Statistical Association* **82**, 371–386.
- Jurek, A. M., Maldonado, G., and Greenland, S. (2013). Adjusting for outcome misclassification: the importance of accounting for case-control sampling and other forms of outcome-related selection. *Annals of Epidemiology* **23**, 129–135.
- Kiefer, T., Diekhoff, T., Hermann, S., Stroux, A., Mews, J., Blobel, J., Hamm, B.,

- and Hermann, K.-G. A. (2016). Single source dual-energy computed tomography in the diagnosis of gout: Diagnostic reliability in comparison to digital radiography and conventional computed tomography of the feet. *European Journal of Radiology* **85**, 1829–1834.
- L. Penning de Vries, B. B. and Groenwold, R. H. H. (2022). Identification of causal effects in case-control studies. *BMC Medical Research Methodology* **22**, 7.
- Lash, T. L. and Fink, A. K. (2003). Semi-automated sensitivity analysis to assess systematic errors in observational data. *Epidemiology* **14**, 451–458.
- Lyles, R. H. and Lin, J. (2010). Sensitivity analysis for misclassification in logistic regression via likelihood methods and predictive value weighting. *Statistics in Medicine* **29**, 2297–2309.
- Månsson, R., Joffe, M. M., Sun, W., and Hennessy, S. (2007). On the estimation and use of propensity scores in case-control and case-cohort studies. *American Journal of Epidemiology* **166**, 332–339.
- Marx, B. D. and Eilers, P. H. (1998). Direct generalized additive modeling with penalized likelihood. *Computational Statistics and Data Analysis* **28**, 193–209.
- Neuhaus, J. M. (1999). Bias and efficiency loss due to misclassified responses in binary regression. *Biometrika* **86**, 843–855.
- Robins, J. M. (1999). Choice as an alternative to control in observational studies: comment. *Statistical Science* **14**, 281–293.
- Rosenbaum, P. R. and Rubin, D. B. (1983). The central role of the propensity score in observational studies for causal effects. *Biometrika* **70**, 41–55.
- Rubin, D. B. (2005). Causal inference using potential outcomes. *Journal of the American Statistical Association* **100**, 322–331.
- Rubin, D. B. and Thomas, N. (2000). Combining propensity score matching with additional

- adjustments for prognostic covariates. *Journal of the American Statistical Association* **95**, 573–585.
- Schlesselman, J. J. (1982). *Case-control Studies: Design, Conduct, Analysis*, volume 2. Oxford University Press, Oxford.
- Shu, D. and Yi, G. Y. (2019a). Causal inference with measurement error in outcomes: Bias analysis and estimation methods. *Statistical Methods in Medical Research* **28**, 2049–2068.
- Shu, D. and Yi, G. Y. (2019b). Weighted causal inference methods with mismeasured covariates and misclassified outcomes. *Statistics in Medicine* **38**, 1835–1854.
- Shu, D. and Yi, G. Y. (2020). Causal inference with noisy data: Bias analysis and estimation approaches to simultaneously addressing missingness and misclassification in binary outcomes. *Statistics in Medicine* **39**, 456–468.
- Van der Laan, M. J. (2008). Estimation based on case-control designs with known prevalence probability. *The International Journal of Biostatistics* **4**, 1–40.
- Van der Laan, M. J. and Rose, S. (2011). *Targeted Learning: Causal Inference for Observational and Experimental Data*, volume 4. Springer, New York.
- Vázquez-Mellado, J., Hernández-Cuevas, C. B., Alvarez-Hernández, E., Ventura-Rios, L., Peláez-Ballestas, I., Casasola-Vargas, J., García-Méndez, S., and Burgos-Vargas, R. (2012). The diagnostic value of the proposal for clinical gout diagnosis (CGD). *Clinical Rheumatology* **31**, 429–434.
- Wacholder, S., Silverman, D. T., McLaughlin, J. K., and Mandel, J. S. (1992). Selection of controls in case-control studies: II. types of controls. *American Journal of Epidemiology* **135**, 1029–1041.
- Yoshida, T. and Naito, K. (2014). Asymptotics for penalised splines in generalised additive models. *Journal of Nonparametric Statistics* **26**, 269–289.

A.1 Proof of Lemma 2.1

Utilizing the law of total probability, we have

$$\begin{aligned}
 \mathbb{P}(Y^* = 1) &= \mathbb{P}(Y^* = 1|Y = 1)\mathbb{P}(Y = 1) + \mathbb{P}(Y^* = 1|Y = 0)\mathbb{P}(Y = 0) \\
 &= \mathbb{P}(Y^* = 1|Y = 1)\mathbb{P}(Y = 1) + \mathbb{P}(Y^* = 1|Y = 0)(1 - \mathbb{P}(Y = 1)) \\
 &= (\mathbb{P}(Y^* = 1|Y = 1) - \mathbb{P}(Y^* = 1|Y = 0))\mathbb{P}(Y = 1) + \mathbb{P}(Y^* = 1|Y = 0).
 \end{aligned}$$

That is $v^* = (p_{11} - p_{01})v + p_{01}$.

Let $s_{01} = \mathbb{P}(S = 1|Y^* = 1)$, $s_{11} = \mathbb{P}(S = 1|Y^* = 0)$. Applying Bayes rule and Assumption 4, we have

$$\begin{aligned}
 s_{11} &= \mathbb{P}(S = 1|Y^* = 1) = \mathbb{P}(Y^* = 1|S = 1) * \mathbb{P}(S = 1) / \mathbb{P}(Y^* = 1), \\
 s_{01} &= \mathbb{P}(S = 1|Y^* = 0) = \mathbb{P}(Y^* = 0|S = 1) * \mathbb{P}(S = 1) / \mathbb{P}(Y^* = 0),
 \end{aligned}$$

thus $s = s_{11}/s_{01} = \frac{\mathbb{P}(Y^*=1|S=1)/v^*}{\mathbb{P}(Y^*=0|S=1)/(1-v^*)}$. Applying Bayes rule,

$$\begin{aligned}
 &\mathbb{P}(Y^* = 1|X, T = 1, S = 1) \\
 &= \frac{\mathbb{P}(Y^* = 1, S = 1|X, T = 1)}{\mathbb{P}(S = 1|X, T = 1)} \\
 &= \frac{\mathbb{P}(S = 1|X, Y^* = 1)\mathbb{P}(Y^* = 1|X, T = 1)}{\mathbb{P}(S = 1|X, Y^* = 1)\mathbb{P}(Y^* = 1|X, T = 1) + \mathbb{P}(S = 1|X, Y^* = 0)\mathbb{P}(Y^* = 0|X, T = 1)} \\
 &= \frac{\mathbb{P}(S = 1|Y^* = 1)\mathbb{P}(Y^* = 1|X, T = 1)}{\mathbb{P}(S = 1|Y^* = 1)\mathbb{P}(Y^* = 1|X, T = 1) + \mathbb{P}(S = 1|Y^* = 0)\mathbb{P}(Y^* = 0|X, T = 1)}.
 \end{aligned}$$

With Assumption 5, it follows:

$$\mathbb{P}(Y^* = 1|X, T = 1) = \frac{s_{01}\mathbb{P}(Y^* = 1|X, T = 1, S = 1)}{s_{11} - \mathbb{P}(Y^* = 1|X, T = 1, S = 1)(s_{11} - s_{01})}. \quad (\text{A.1})$$

We also have

$$\begin{aligned}
 \mathbb{P}(Y^* = 1|X, T = 1) &= \mathbb{P}(Y^* = 1|X, Y = 1, T = 1)\mathbb{P}(Y = 1|X, T = 1) \\
 &\quad + \mathbb{P}(Y^* = 1|X, Y = 0, T = 1)\mathbb{P}(Y = 0|X, T = 1) \\
 &= \mathbb{P}(Y^* = 1|Y = 1)\mathbb{P}(Y = 1|X, T = 1) \\
 &\quad + \mathbb{P}(Y^* = 1|Y = 0)\mathbb{P}(Y = 0|X, T = 1),
 \end{aligned}$$

which follows that

$$\mathbb{P}(Y = 1|X, T = 1) = \frac{\mathbb{P}(Y^* = 1|X, T = 1) - p_{01}}{p_{11} - p_{01}}. \quad (\text{A.2})$$

With (A.1) and (A.2), we obtain

$$g_1(X) = \mathbb{E}[Y|X, T = 1] = \frac{1}{p_{11} - p_{01}} \left(\frac{s_{01}g_1^*(X)}{s_{11} - g_1^*(X)(s_{11} - s_{01})} - p_{01} \right)$$

Analogously, we have

$$g_0(X) = \mathbb{E}[Y|X, T = 1] = \frac{1}{p_{11} - p_{01}} \left(\frac{s_{01}g_0^*(X)}{s_{11} - g_0^*(X)(s_{11} - s_{01})} - p_{01} \right).$$

A.2 Proof of Theorem 3.1

A.2.1 Notations.

Let $\boldsymbol{\theta}_0$ denote the true parameter values for $\boldsymbol{\theta}$. Let $\boldsymbol{\psi}'(\boldsymbol{\theta})$ denote $\partial\boldsymbol{\psi}(Y^*, X, T, \boldsymbol{\theta})/\partial\boldsymbol{\theta}^\top$ and $\boldsymbol{\psi}''(\boldsymbol{\theta})$ denote $\partial^2\boldsymbol{\psi}(Y^*, X, T, \boldsymbol{\theta})/\partial\boldsymbol{\theta}\partial\boldsymbol{\theta}^\top$. Let $\mathbf{H}(\boldsymbol{\theta})$ denote $\mathbb{E}\{\boldsymbol{\psi}'(Y^*, X, T, \boldsymbol{\theta}) | S = 1\}$ and $\mathbf{B}(\boldsymbol{\theta})$ denote $\mathbb{E}\left\{\boldsymbol{\psi}(Y^*, X, T, \boldsymbol{\theta})\boldsymbol{\psi}(Y^*, X, T, \boldsymbol{\theta})^\top | S = 1\right\}$.

A.2.2 Regularity conditions for Theorem 3.1.

(A1) Assume that $\boldsymbol{\psi}'(\boldsymbol{\theta})$ and $\boldsymbol{\psi}''(\boldsymbol{\theta})$ exist and uniformly bounded for all $\boldsymbol{\theta}$ in an open neighborhood of $\boldsymbol{\theta}_0$.

(A2) $\mathbf{H}(\boldsymbol{\theta}_0)$ and $\mathbf{B}(\boldsymbol{\theta}_0)$ are positive definite.

A.2.3 Proof of Theorem 3.1.

By standard Z-estimation theory and $\mathbb{E}[\boldsymbol{\psi}(\boldsymbol{\theta}_0) | S = 1] = \mathbf{0}$, a solution $\hat{\boldsymbol{\theta}}$ to the estimating equation $\boldsymbol{\psi}(\boldsymbol{\theta}) = \mathbf{0}$, exists, unique, and consistent, i.e., $\hat{\boldsymbol{\theta}} \xrightarrow{p} \boldsymbol{\theta}_0$. To establish asymptotic normality, the estimators $\hat{\boldsymbol{\theta}}$ solve the equation

$$\boldsymbol{\Psi}_n(\hat{\boldsymbol{\theta}}) := \frac{1}{n} \sum_{i=1}^n \boldsymbol{\psi}(y_i^*, x_i, t_i, \hat{\boldsymbol{\theta}}) = \mathbf{0}.$$

Taking Taylor expansion of $\boldsymbol{\Psi}_n(\hat{\boldsymbol{\theta}})$, we have

$$\mathbf{0} = \boldsymbol{\Psi}_n(\hat{\boldsymbol{\theta}}) = \boldsymbol{\Psi}_n(\boldsymbol{\theta}_0) + \boldsymbol{\Psi}'_n(\boldsymbol{\theta}_0) (\hat{\boldsymbol{\theta}} - \boldsymbol{\theta}_0) + \mathbf{R}_n.$$

where $\boldsymbol{\Psi}'_n(\boldsymbol{\theta}_0) = -\partial\boldsymbol{\Psi}_n(\boldsymbol{\theta})/\partial\boldsymbol{\theta}^\top|_{\boldsymbol{\theta}=\boldsymbol{\theta}_0}$. Under regularity conditions specified above, $-\boldsymbol{\Psi}'_n(\boldsymbol{\theta}_0) \xrightarrow{p} \mathbf{H}(\boldsymbol{\theta}_0)$ and $\sqrt{n}\mathbf{R}_n \xrightarrow{p} 0$ as $n \rightarrow \infty$, so that

$$\sqrt{n}(\hat{\boldsymbol{\theta}} - \boldsymbol{\theta}_0) \approx \mathbf{H}^{-1}(\boldsymbol{\theta}_0) \sqrt{n}\boldsymbol{\Psi}_n(\boldsymbol{\theta}_0).$$

By applying the Central Limit Theorem,

$$\sqrt{n}\boldsymbol{\Psi}_n(\boldsymbol{\theta}_0) \xrightarrow{d} N\{\mathbf{0}, \mathbf{B}(\boldsymbol{\theta}_0)\}.$$

Therefore, we have that

$$\sqrt{n}(\hat{\boldsymbol{\theta}} - \boldsymbol{\theta}_0) \sim N\left(\mathbf{0}, \mathbf{H}(\boldsymbol{\theta}_0)^{-1} \mathbf{B}(\boldsymbol{\theta}_0) \{\mathbf{H}(\boldsymbol{\theta}_0)^{-1}\}^\top\right) \text{ as } n \rightarrow \infty$$

A.3 Proof of Theorem 3.2

A.3.1 Notations.

As denoted in Section 3, for i -th individual, $\mathbf{Z}_i = (\mathbf{B}(x_{i1})^\top, \dots, \mathbf{B}(x_{iD})^\top, T_i)$, where $\mathbf{B}(x) = (B_{-p+1}(x), \dots, B_{K_n}(x))^\top$, $\boldsymbol{\beta}^\top = (\mathbf{b}^\top, a)$, $\mathbf{b}^\top = (\mathbf{b}_1^\top, \dots, \mathbf{b}_D^\top)$ and $\mathbf{b}_j = \{b_{k,j}\}_{k=-p+1}^{K_n}$, $j = 1, \dots, D$. The explicit expressions for the estimating equations are provided below:

$$\boldsymbol{\Psi}_n(\boldsymbol{\theta}, \lambda_n, \gamma_n) := \frac{1}{n} \sum_i^n \boldsymbol{\psi}(y_i^*, x_i, t_i, \boldsymbol{\theta}, \lambda_n, \gamma_n) = \begin{pmatrix} S_n(s) \\ G_{\text{rp},n}(\boldsymbol{\beta}, s, \lambda_n, \gamma_n) \\ M_n(\eta(\boldsymbol{\beta}), \mathbf{u}) \end{pmatrix},$$

where

$$S_n(s) = \frac{1}{n} \sum_{i=1}^n \{sv^*(1 - y_i^*) - (1 - v^*)y_i^*\} = 0,$$

$$G_{\text{rp},n}(\boldsymbol{\beta}, s, \lambda_n, \gamma_n) = \frac{\partial \ell_{\text{rp},n}(\boldsymbol{\beta}, s, \lambda_n, \gamma_n)}{\partial \boldsymbol{\beta}} = \frac{1}{n} \mathbf{Z}^\top U(\eta(\boldsymbol{\beta}), s) - \frac{1}{n} Q_m^a(\lambda_n) \boldsymbol{\beta} - \frac{1}{n} T^a(\gamma_n) \boldsymbol{\beta},$$

$$M_n(\eta(\boldsymbol{\beta}), \mathbf{u}) = \frac{1}{n} \sum_{i=1}^n \begin{pmatrix} y_i^*(u_{11} - \text{expit}(\eta(T=1, X = \mathbf{x}_i, \boldsymbol{\beta}))) \\ (1 - y_i^*)(u_{10} - \text{expit}(\eta(T=1, X = \mathbf{x}_i, \boldsymbol{\beta}))) \\ y_i^*(u_{01} - \text{expit}(\eta(T=0, X = \mathbf{x}_i, \boldsymbol{\beta}))) \\ (1 - y_i^*)(u_{00} - \text{expit}(\eta(T=0, X = \mathbf{x}_i, \boldsymbol{\beta}))) \end{pmatrix},$$

$$U(\eta(\boldsymbol{\beta}), s) = \left\{ (Y_i - h(\eta(\mathbf{Z}_i, \boldsymbol{\beta}))) \frac{h'(\eta(\mathbf{Z}_i, \boldsymbol{\beta}))}{h(\eta(\mathbf{Z}_i, \boldsymbol{\beta}))(1 - h(\eta(\mathbf{Z}_i, \boldsymbol{\beta})))} \right\}_{\{i=1, \dots, n\}},$$

$$Q_m^a(\lambda_n) = \begin{bmatrix} Q_m(\lambda_n) & 0 \\ 0 & 0 \end{bmatrix}, T^a(\gamma_n) = \begin{bmatrix} \gamma_n I & 0 \\ 0 & 0 \end{bmatrix}, Q_m(\lambda_n) = \text{diag}[\lambda_{1n} \Delta_m^\top \Delta_m \dots \lambda_{Dn} \Delta_m^\top \Delta_m].$$

Note that only the spline parameters \mathbf{b}_j , $j = 1, \dots, D$ are penalized. The Hessian matrix can be written as:

$$\mathbf{H}_n(\boldsymbol{\theta}, \lambda_n, \gamma_n) := \boldsymbol{\Psi}'_n(\boldsymbol{\theta}, \lambda_n, \gamma_n) = \begin{bmatrix} \mathbf{H}_{n,1}(s) & 0 & 0 \\ \mathbf{H}_{n,2}(\boldsymbol{\beta}, s) & \mathbf{H}_{n,3}(\boldsymbol{\beta}, s) & 0 \\ 0 & \mathbf{H}_{n,4}(\mathbf{u}, \boldsymbol{\beta}) & \mathbf{H}_{n,5} \end{bmatrix}, \quad (\text{A.3})$$

where

(A.4)

$$\begin{aligned}\mathbf{H}_{n,1}(s) &= \frac{\partial S_n(s)}{\partial s}, & \mathbf{H}_{n,2}(\boldsymbol{\beta}, s) &= \frac{\partial G_{rp,n}(\boldsymbol{\beta}, s)}{\partial s}, \\ \mathbf{H}_{n,3}(\boldsymbol{\beta}, s) &= \frac{\partial G_{rp,n}(\boldsymbol{\beta}, s)}{\partial \boldsymbol{\beta}} = -\frac{1}{n} \mathbf{Z}^\top W(\eta(\boldsymbol{\beta}), s) \mathbf{Z} - \frac{1}{n} Q_m^a(\lambda_n) - \frac{1}{n} T^a(\gamma_n), \\ \mathbf{H}_{n,4}(\boldsymbol{\beta}, \mathbf{u}) &= \frac{\partial M_n(\eta(\boldsymbol{\beta}), \mathbf{u})}{\partial \boldsymbol{\beta}}, & \mathbf{H}_{n,5} &= \frac{\partial M_n(\eta(\boldsymbol{\beta}), \mathbf{u})}{\partial \mathbf{u}}.\end{aligned}$$

and $W(\eta(\boldsymbol{\beta}), s) = \text{diag}[w_i(\eta(\mathbf{Z}_i, \boldsymbol{\beta}), s)]$ is a n -dimensional diagonal weight matrix resulting from the variance function, with

$$w_i = \frac{h'(\eta(\mathbf{Z}_i, \boldsymbol{\beta}))^2}{V(\eta(\mathbf{Z}_i, \boldsymbol{\beta}))} - \{Y_i - h(\eta(\mathbf{Z}_i, \boldsymbol{\beta}))\} \frac{h''(\eta(\mathbf{Z}_i, \boldsymbol{\beta}))V(\eta(\mathbf{Z}_i, \boldsymbol{\beta})) - h'(\eta(\mathbf{Z}_i, \boldsymbol{\beta}))^2 V'(\eta(\mathbf{Z}_i, \boldsymbol{\beta}))}{V(\eta(\mathbf{Z}_i, \boldsymbol{\beta}))^2},$$

$$V(\eta(\mathbf{Z}_i, \boldsymbol{\beta})) = h(\eta(\mathbf{Z}_i, \boldsymbol{\beta}))(1 - h(\eta(\mathbf{Z}_i, \boldsymbol{\beta}))).$$

We further define

$$\tilde{\Psi}_n(\boldsymbol{\theta}, \lambda_n, \gamma_n) := \frac{1}{n} \sum_i^n \tilde{\psi}(y_i^*, x_i, t_i, \boldsymbol{\theta}, \lambda_n, \gamma_n) := \begin{pmatrix} S_n(s) \\ \tilde{G}_{rp,n}(\boldsymbol{\beta}, s, \lambda_n, \gamma_n) \\ \tilde{M}_n(\mathbf{u}) \end{pmatrix}, \quad (\text{A.5})$$

$$\tilde{G}_{rp,n}(\boldsymbol{\beta}, s, \lambda_n, \gamma_n) = \frac{1}{n} \mathbf{Z}^\top U(\tilde{\eta}, s) - \frac{1}{n} Q_m^a(\lambda_n) \boldsymbol{\beta} - \frac{1}{n} T^a(\gamma_n) \boldsymbol{\beta},$$

$$\tilde{M}_n(\mathbf{u}) = \frac{1}{n} \sum_{i=1}^n \begin{pmatrix} y_i^*(u_{11} - \text{expit}(\tilde{\eta}(T=1, X=\mathbf{x}_i))) \\ (1 - y_i^*)(u_{10} - \text{expit}(\tilde{\eta}(T=1, X=\mathbf{x}_i))) \\ y_i^*(u_{01} - \text{expit}(\tilde{\eta}(T=0, X=\mathbf{x}_i))) \\ (1 - y_i^*)(u_{00} - \text{expit}(\tilde{\eta}(T=0, X=\mathbf{x}_i))) \end{pmatrix}.$$

The definition of $\tilde{\mathbf{H}}_n(\boldsymbol{\theta}, \lambda_n, \gamma_n)$ is similar:

$$\tilde{\mathbf{H}}_n(\boldsymbol{\theta}, \lambda_n, \gamma_n) := \frac{1}{n} \sum_i^n \tilde{\psi}'(y_i^*, x_i, t_i, \boldsymbol{\theta}, \lambda_n, \gamma_n) := \begin{bmatrix} \mathbf{H}_{n,1}(s) & 0 & 0 \\ \tilde{\mathbf{H}}_{n,2}(s) & \tilde{\mathbf{H}}_{n,3}(s) & 0 \\ 0 & \tilde{\mathbf{H}}_{n,4} & \mathbf{H}_{n,5} \end{bmatrix}, \quad (\text{A.6})$$

where

$$\begin{aligned}\tilde{\mathbf{H}}_{n,2}(s) &= \frac{1}{n} \mathbf{Z}^\top \partial U(\tilde{\eta}, s) / \partial s, \\ \tilde{\mathbf{H}}_{n,3}(s) &= -\frac{1}{n} \mathbf{Z}^\top W(\tilde{\eta}, s) \mathbf{Z} - \frac{1}{n} Q_m^a(\lambda_n) - \frac{1}{n} T^a(\gamma_n), \\ \tilde{\mathbf{H}}_{n,4} &= \frac{1}{n} \sum_{i=1}^n \begin{pmatrix} y_i^* \text{expit}'(\tilde{\eta}(T=1, X=\mathbf{x}_i)) \mathbf{Z}_i^\top \\ (1-y_i^*) \text{expit}'(\tilde{\eta}(T=1, X=\mathbf{x}_i)) \mathbf{Z}_i^\top \\ -y_i^* \text{expit}'(\tilde{\eta}(T=0, X=\mathbf{x}_i)) \mathbf{Z}_i^\top \\ (1-y_i^*) \text{expit}'(\tilde{\eta}(T=0, X=\mathbf{x}_i)) \mathbf{Z}_i^\top \end{pmatrix}.\end{aligned}$$

To simplify notation, we rewrite $\tilde{\mathbf{H}}_n(\boldsymbol{\theta}, \lambda_n, \gamma_n)$ as $\tilde{\Psi}'_n(s, \lambda_n, \gamma_n)$.

Let $\boldsymbol{\theta}_0 = (s_0, \boldsymbol{\beta}_0^\top, \mathbf{u}_0^\top)^\top$, where s_0 is the solution of $\mathbb{E}[S_n(s)|S=1] = 0$, $\boldsymbol{\beta}_0 = (\mathbf{b}_0^\top, a_0)^\top = \underset{\boldsymbol{\beta}}{\text{argmin}} \mathbb{E} \left[\log \frac{f(Y, \mathbf{X}, \tilde{\eta})}{f(Y, \mathbf{X}, \boldsymbol{\beta})} | S=1 \right]$ is the best spline approximation of true index function $\tilde{\eta}(t, \mathbf{x})$ based on Kullback-Leibler measure and \mathbf{u}_0 is the solution of $\mathbb{E}[M_n(\mathbf{u}, \boldsymbol{\beta}_0)|S=1] = 0$. Let $\tau_0 = \mathbb{E}[\text{expit}(\eta_0(T=1, X)) - \text{expit}(\eta_0(T=0, X))]$, where $\eta_0(t, \mathbf{x}) = \mathbf{Z}\boldsymbol{\beta}_0$. Define

$$\begin{aligned}\tilde{\mathbf{H}}(\lambda_n) &= \mathbb{E} \left\{ \tilde{\Psi}'_n(\boldsymbol{\theta}_0, \lambda_n, \gamma_n = 0) | S=1 \right\}, \\ \tilde{\mathbf{B}} &= n \mathbb{E} \left\{ \tilde{\Psi}_n(\boldsymbol{\theta}_0, \lambda_n, \gamma_n = 0) \Psi_n(\boldsymbol{\theta}_0, \lambda_n, \gamma_n = 0)^\top | S=1 \right\}.\end{aligned}$$

Noting that

$$\begin{aligned}\tilde{\mathbf{H}}(\lambda_n) &= \mathbb{E} \left\{ \tilde{\psi}'(Y^*, X, T, \boldsymbol{\theta}_0, \lambda_n, \gamma_n = 0) | S=1 \right\}, \\ \tilde{\mathbf{B}} &= \mathbb{E} \left\{ \tilde{\psi}(Y^*, X, T, \boldsymbol{\theta}_0, \lambda_n = 0, \gamma_n = 0) \tilde{\psi}(Y^*, X, T, \boldsymbol{\theta}_0, \lambda_n = 0, \gamma_n = 0)^\top | S=1 \right\}.\end{aligned}$$

A.3.2 Regularity conditions for Theorem 3.2.

To give the asymptotic properties of $\hat{\tau}_{\text{GAM}}$, we make the following assumptions:

(B1) We assume that the covariate points $\mathbf{x}_i = (x_{i1}, \dots, x_{iD})$ are distributed according to a density with compact support on $[0, 1]^D$, where $[0, 1]^D$ is the D -variate unit cube.

(B2) For simplicity, the knots for the B-spline basis are equidistantly located so that $\kappa_k = k/K_n (k = -p+1, \dots, K_n+p)$ with $\kappa_j - \kappa_{j-1} = O(K_n^{-1})$ for $j = -p+1, \dots, K_n+p$.

(B3) The smoothing parameter is often chosen as $\lambda_{jn} \rightarrow \infty$ with $n \rightarrow \infty$ because a

spline curve often yields overfitting for large n . Thus we assume the penalty parameter $\lambda_{jn}(j = 1, \dots, D)$ grow with the sample size with order

$$\lambda_{jn} = o(nK_n^{-1}).$$

(B4) We assume that the dimension of the B-spline basis grows with the sample size with order

$$K_n = o(n^{1/2}).$$

and for the non-singularity of $\mathbf{H}_{n,3}(\boldsymbol{\theta}, \lambda_n, \gamma_n)$, K_n is chosen such that $D(K_n + p) + 1 < n$.

(B5) The ridge corrected penalty satisfies $\gamma = o(\lambda_n K_n^{-m})$, where $\lambda_n = \max_j \lambda_{jn}$.

Moreover, the function $\tilde{\eta}_j(j = 1, \dots, D)$ is assumed to be $(p+1)$ times differentiable and expects a finite number of isolated points in $[0,1]$ it is continuously differentiable. This guarantees that the likelihood contributions are all of the same asymptotic order $O_p(\mathbf{1})$.

A.3.3 Lemmas for Theorem 3.2.

Before the proof of theorem 3.2, We give several lemmas as follows:

Lemma B1 Under Assumptions B1-B5, we have

$$\hat{\boldsymbol{\beta}} - \boldsymbol{\beta}_0 = -\mathbf{H}_{n,3}(\boldsymbol{\beta}_0, s_0, \lambda_n, \gamma_n)^{-1} G_{\text{rp},n}(\boldsymbol{\beta}_0, s_0, \lambda_n, \gamma_n) + o_p \left(\left\{ \left(\frac{\lambda_n K_n^{1-m}}{n} \right)^2 + \frac{K_n}{n} \right\} \mathbf{1} \right).$$

Lemma B2 Under Assumptions B1-B5, we have

$$\tilde{\eta}(\mathbf{x}) - \eta_0(\mathbf{x}) = b_a(\mathbf{x}) + o(K_n^{-(p+1)})$$

where $b_a(\mathbf{x}) = \sum_{j=1}^D b_{j,a}(x_j)$,

$$b_{j,a}(x) = \frac{\tilde{\eta}_j^{(p+1)}(x)}{K_n^{p+1}(p+1)!} \sum_{k=1}^{K_n} I(\kappa_{k-1} \leq x < \kappa_k) \text{Br}_{p+1} \left(\frac{x - \kappa_{k-1}}{K_n^{-1}} \right), \quad (\text{A.7})$$

and $I(a < x < b)$ is the indicator function of an interval (a, b) and $\text{Br}_p(x)$ is the p -th Bernoulli polynomial.

A.3.4 Proof of Theorem 3.2.

To assess the difference between $(\hat{\tau}_{\text{GAM}} - \tau)$, we decompose it into two distinct components:

$(\hat{\tau}_{\text{GAM}} - \tau_0)$ and $(\tau_0 - \tau)$ and evaluate them by the following steps. **Step 1**, we establish the asymptotic properties of $\hat{\boldsymbol{\theta}} - \boldsymbol{\theta}_0$. **Step 2**, we determine the asymptotic order of $\mathbb{E}(\hat{\boldsymbol{\theta}} - \boldsymbol{\theta}_0 | S = 1)$ and $\mathbb{V}(\hat{\boldsymbol{\theta}} - \boldsymbol{\theta}_0 | S = 1)$. **Step 3**, we establish the asymptotic properties of $(\hat{\tau}_{\text{GAM}} - \tau_0)$. **Step 4**, we evaluate $(\tau - \tau_0)$.

Step 1: we first prove that

$$\hat{\boldsymbol{\theta}} - \boldsymbol{\theta}_0 = -\mathbf{H}_n(\boldsymbol{\theta}_0, \lambda_n, \gamma_n)^{-1} \boldsymbol{\Psi}_n(\boldsymbol{\theta}_0, \lambda_n, \gamma_n) + O_p\left(\left\{\left(\frac{\lambda_n K_n^{1-m}}{n}\right)^2 + \frac{K_n}{n}\right\} \mathbf{1}\right). \quad (\text{A.8})$$

Taking Taylor's expansion of $\boldsymbol{\Psi}_n(\hat{\boldsymbol{\theta}}, \lambda_n, \gamma_n)$ around $\boldsymbol{\theta}_0$, we have

$$\begin{aligned} 0 &= \boldsymbol{\Psi}_n(\hat{\boldsymbol{\theta}}, \lambda_n, \gamma_n) \\ &= \boldsymbol{\Psi}_n(\boldsymbol{\theta}_0, \lambda_n, \gamma_n) + \mathbf{H}_n(\boldsymbol{\theta}_0, \lambda_n, \gamma_n) (\hat{\boldsymbol{\theta}} - \boldsymbol{\theta}_0) \\ &\quad + \left\{ \mathbf{H}_n(\boldsymbol{\theta}_0 + \Omega (\hat{\boldsymbol{\theta}} - \boldsymbol{\theta}_0), \lambda_n, \gamma_n) - \mathbf{H}_n(\boldsymbol{\theta}_0, \lambda_n, \gamma_n) \right\} (\hat{\boldsymbol{\theta}} - \boldsymbol{\theta}_0), \end{aligned}$$

where $\Omega = \text{diag}[\omega_1, \dots, \omega_{D(K_n+p)}, \omega_a]$ and $\omega_i \in (0, 1)$. To simplify notation, the tuning parameters λ_n and γ_n are omitted in the subsequent proof. By simple calculation, we rewrite the difference:

$$\begin{aligned} &\mathbf{H}_n(\boldsymbol{\theta}_0 + \Omega (\hat{\boldsymbol{\theta}} - \boldsymbol{\theta}_0)) - \mathbf{H}_n(\boldsymbol{\theta}_0) \\ &= \begin{bmatrix} 0 & & 0 & & 0 \\ \mathbf{H}_{n,2}(\boldsymbol{\theta}_0 + \Omega (\hat{\boldsymbol{\theta}} - \boldsymbol{\theta}_0)) - \mathbf{H}_{n,2}(\boldsymbol{\theta}_0) & \mathbf{H}_{n,3}(\boldsymbol{\theta}_0 + \Omega (\hat{\boldsymbol{\theta}} - \boldsymbol{\theta}_0)) - \mathbf{H}_{n,3}(\boldsymbol{\theta}_0) & 0 \\ 0 & \mathbf{H}_{n,4}(\boldsymbol{\theta}_0 + \Omega (\hat{\boldsymbol{\theta}} - \boldsymbol{\theta}_0)) - \mathbf{H}_{n,4}(\boldsymbol{\theta}_0) & 0 \end{bmatrix} \\ &=: \begin{bmatrix} 0 & 0 & 0 \\ \Delta \mathbf{H}_{n,2} & \Delta \mathbf{H}_{n,3} & 0 \\ 0 & \Delta \mathbf{H}_{n,4} & 0 \end{bmatrix}, \end{aligned}$$

We also calculate the inverse of $\mathbf{H}_n(\boldsymbol{\theta}_0)$:

$$\mathbf{H}_n(\boldsymbol{\theta}_0)^{-1} = \begin{bmatrix} \mathbf{H}_{n,1}^{-1} & 0 & 0 \\ -\mathbf{H}_{n,3}^{-1} \mathbf{H}_{n,2} \mathbf{H}_{n,1}^{-1} & \mathbf{H}_{n,3}^{-1} & 0 \\ \mathbf{H}_{n,5}^{-1} \mathbf{H}_{n,4} \mathbf{H}_{n,3}^{-1} \mathbf{H}_{n,2} \mathbf{H}_{n,1}^{-1} & -\mathbf{H}_{n,5}^{-1} \mathbf{H}_{n,4} \mathbf{H}_{n,3}^{-1} & \mathbf{H}_{n,5}^{-1} \end{bmatrix},$$

Thus we have

$$\begin{aligned}
& \hat{\boldsymbol{\theta}} - \boldsymbol{\theta}_0 \\
&= -\mathbf{H}_n(\boldsymbol{\theta}_0)^{-1} \boldsymbol{\Psi}_n(\boldsymbol{\theta}_0) - \mathbf{H}_n(\boldsymbol{\theta}_0)^{-1} \begin{bmatrix} 0 & 0 & 0 \\ \Delta\mathbf{H}_{n,2} & \Delta\mathbf{H}_{n,3} & 0 \\ 0 & \Delta\mathbf{H}_{n,4} & 0 \end{bmatrix} (\hat{\boldsymbol{\theta}} - \boldsymbol{\theta}_0) \\
&= -\mathbf{H}_n(\boldsymbol{\theta}_0)^{-1} \boldsymbol{\Psi}_n(\boldsymbol{\theta}_0) \\
&+ \begin{bmatrix} 0 \\ -\mathbf{H}_{n,3}^{-1} \Delta\mathbf{H}_{n,2} (\hat{s} - s_0) - \mathbf{H}_{n,3}^{-1} \Delta\mathbf{H}_{n,3} (\hat{\boldsymbol{\beta}} - \boldsymbol{\beta}_0) \\ \mathbf{H}_{n,5}^{-1} \mathbf{H}_{n,4} \mathbf{H}_{n,3}^{-1} \Delta\mathbf{H}_{n,2} (\hat{s} - s_0) - (\mathbf{H}_{n,5}^{-1} \Delta\mathbf{H}_{n,4} - \mathbf{H}_{n,5}^{-1} \mathbf{H}_{n,4} \mathbf{H}_{n,3}^{-1} \Delta\mathbf{H}_{n,3}) (\hat{\boldsymbol{\beta}} - \boldsymbol{\beta}_0) \end{bmatrix}.
\end{aligned}$$

According to Lemma A.1-A.3 given by Yoshida and Naito (2014), we can easily obtain that

$$\begin{aligned}
\mathbf{H}_{n,3} &= O_p(K_n^{-1} \mathbf{1}\mathbf{1}^\top), \\
\mathbf{H}_{n,3}^{-1} \Delta\mathbf{H}_{n,3} &= o_p \left(\left\{ \frac{\lambda_n K_n^{1-m}}{n} + \sqrt{\frac{K_n}{n}} \right\} \mathbf{1}\mathbf{1}^\top \right).
\end{aligned}$$

It is worth noting that $\partial U(\eta(\beta), s)/\partial s$ is continuously differentiable up to the $(p+1)$ -th order with respect to s , and uniformly bounded for $s \geq 1$. Through straightforward calculations, it can be demonstrated that

$$\begin{aligned}
\mathbf{H}_{n,2} &= O_p(K_n^{-1} \mathbf{1}), \quad \mathbf{H}_{n,4} = O_p(K_n^{-1} \mathbf{1}\mathbf{1}^\top), \\
\Delta\mathbf{H}_{n,4} &= O_p \left(\left\{ \frac{\lambda_n K_n^{1-m}}{n} + \sqrt{\frac{K_n}{n}} \right\} \mathbf{1}\mathbf{1}^\top \right).
\end{aligned}$$

What's more, it can be easily derived that $\hat{s} - s_0 = O_p(1/\sqrt{n})$. Based on all the aforementioned results and Lemma B1, we have

$$\begin{aligned}
& -\mathbf{H}_{n,3}^{-1} \Delta\mathbf{H}_{n,2} (\hat{s} - s_0) - \mathbf{H}_{n,3}^{-1} \Delta\mathbf{H}_{n,3} (\hat{\boldsymbol{\beta}} - \boldsymbol{\beta}_0) = o_p \left(\left\{ \left(\frac{\lambda_n K_n^{1-m}}{n} \right)^2 + \frac{K_n}{n} \right\} \mathbf{1} \right), \\
& \mathbf{H}_{n,5}^{-1} \mathbf{H}_{n,4} \mathbf{H}_{n,3}^{-1} \Delta\mathbf{H}_{n,2} (\hat{s} - s_0) - (\mathbf{H}_{n,5}^{-1} \Delta\mathbf{H}_{n,4} - \mathbf{H}_{n,5}^{-1} \mathbf{H}_{n,4} \mathbf{H}_{n,3}^{-1} \Delta\mathbf{H}_{n,3}) (\hat{\boldsymbol{\beta}} - \boldsymbol{\beta}_0) \\
&= O_p \left(\left\{ \left(\frac{\lambda_n K_n^{1-m}}{n} \right)^2 + \frac{K_n}{n} \right\} \mathbf{1} \right).
\end{aligned}$$

The proof of **Step 1** is finished.

Step 2: We next calculate the order of $\mathbb{E}(\hat{\boldsymbol{\theta}} - \boldsymbol{\theta}_0 | S = 1)$ and $\mathbf{V}(\hat{\boldsymbol{\theta}} - \boldsymbol{\theta}_0 | S = 1)$.

According to LLN, it can be proved that

$$\mathbf{H}_n(\boldsymbol{\theta}_0)^{-1} = \tilde{\mathbf{H}}(\lambda_n)^{-1} (1 + o_p(\mathbf{1}\mathbf{1}^\top)).$$

Thus we have

$$\begin{aligned} \hat{\boldsymbol{\theta}} - \boldsymbol{\theta}_0 &= -\mathbf{H}_n(\boldsymbol{\theta}_0)^{-1} \boldsymbol{\Psi}_n(\boldsymbol{\theta}_0) + O_p\left(\left\{\left(\frac{\lambda_n K_n^{1-m}}{n}\right)^2 + \frac{K_n}{n}\right\} \mathbf{1}\right) \\ &= -\tilde{\mathbf{H}}(\lambda_n)^{-1} (1 + o_p(\mathbf{1}\mathbf{1}^\top)) \boldsymbol{\Psi}_n(\boldsymbol{\theta}_0) + O_p\left(\left\{\left(\frac{\lambda_n K_n^{1-m}}{n}\right)^2 + \frac{K_n}{n}\right\} \mathbf{1}\right) \\ &= -\tilde{\mathbf{H}}(\lambda_n)^{-1} \boldsymbol{\Psi}_n(\boldsymbol{\theta}_0) + o_p\left(\left\{\frac{\lambda_n K_n^{1-m}}{n} + \sqrt{\frac{K_n}{n}}\right\} \mathbf{1}\right). \end{aligned} \quad (\text{A.9})$$

Taking the expectation on both sides of the equation, we obtain

$$\begin{aligned} \mathbb{E}(\hat{\boldsymbol{\theta}} - \boldsymbol{\theta}_0 | S = 1) &= -\tilde{\mathbf{H}}(\lambda_n)^{-1} \mathbb{E}(\boldsymbol{\Psi}_n(\boldsymbol{\theta}_0)) + o\left(\left\{\frac{\lambda_n K_n^{1-m}}{n} + \sqrt{\frac{K_n}{n}}\right\} \mathbf{1}\right) \\ &= -\tilde{\mathbf{H}}(\lambda_n)^{-1} \mathbb{E}\left(\begin{bmatrix} \mathbf{S}_n(s_0) \\ \mathbf{G}_{rp,n}(\boldsymbol{\beta}_0, s_0) \\ \mathbf{M}_n(\mathbf{u}_0, \boldsymbol{\beta}_0) \end{bmatrix}\right) + o\left(\left\{\frac{\lambda_n K_n^{1-m}}{n} + \sqrt{\frac{K_n}{n}}\right\} \mathbf{1}\right) \\ &= -\tilde{\mathbf{H}}(\lambda_n)^{-1} \begin{bmatrix} 0 \\ -\frac{1}{n} Q_m(\lambda_n) \boldsymbol{\beta}_0 - \frac{\gamma_m}{n} \boldsymbol{\beta}_0 \\ 0 \end{bmatrix} + o\left(\left\{\frac{\lambda_n K_n^{1-m}}{n} + \sqrt{\frac{K_n}{n}}\right\} \mathbf{1}\right) \\ &= O\left(\left\{\frac{\lambda_n K_n^{1-m}}{n}\right\} \mathbf{1}\right) + o\left(\left\{\sqrt{\frac{K_n}{n}}\right\} \mathbf{1}\right). \end{aligned}$$

Here, we have used the fact:

$$\begin{aligned} \left(\frac{\gamma_n}{n}\right) \tilde{\mathbf{H}}_{n,3}^{-1} \boldsymbol{\beta}_0 &= o(\lambda_n K_n^{1-m} n^{-1} \mathbf{1}), \\ \left(\frac{\gamma_n}{n}\right) \tilde{\mathbf{H}}_{n,4} \tilde{\mathbf{H}}_{n,3}^{-1} \boldsymbol{\beta}_0 &= o(\lambda_n K_n^{1-m} n^{-1}). \end{aligned}$$

According to (A.9) and LLN, we have

$$\mathbb{V}(\boldsymbol{\Psi}_n(\boldsymbol{\theta}_0) | S = 1) = \frac{1}{n} \tilde{\mathbf{B}} (1 + o_p(\mathbf{1}\mathbf{1}^\top)),$$

$$\mathbb{V}\left(\hat{\boldsymbol{\theta}} - \boldsymbol{\theta}_0 | S = 1\right) = \frac{1}{n} \tilde{\mathbf{H}}(\lambda_n)^{-1} \tilde{\mathbf{B}} \left\{ \tilde{\mathbf{H}}(\lambda_n)^{-1} \right\}^\top + o\left(\frac{K_n}{n}\right) = O\left(\frac{K_n}{n}\right), \quad (\text{A.10})$$

where

$$\tilde{\mathbf{B}} = \mathbb{E} \left\{ \tilde{\boldsymbol{\psi}}(Y^*, X, T, \boldsymbol{\theta}_0, \lambda_n = 0, \gamma_n = 0) \tilde{\boldsymbol{\psi}}(Y^*, X, T, \boldsymbol{\theta}_0, \lambda_n = 0, \gamma_n = 0)^\top | S = 1 \right\}.$$

Step 3: We give the asymptotic normality of the difference $(\hat{\tau}_{\text{GAM}} - \tau_0)$.

Let $\mathbf{c} = (c_{11}, c_{10}, c_{01}, c_{00})^\top$ and $\mathbf{q} = (\mathbf{0}^\top, \mathbf{c}^\top)^\top$, we have $\hat{\tau}_{\text{GAM}} = \mathbf{q}^\top \hat{\boldsymbol{\theta}}$. Thus applying the CLT and the Slutsky formula we obtain:

$$\hat{\tau}_{\text{GAM}} - \tau_0 \stackrel{a}{\sim} \mathcal{N}(\text{Bias}_\lambda(\hat{\tau}_{\text{GAM}}), \mathbf{V}(\hat{\tau}_{\text{GAM}})),$$

where

$$\text{Bias}_\lambda(\hat{\tau}_{\text{GAM}}) = \mathbf{q}^\top \text{Bias}(\hat{\boldsymbol{\theta}}), \quad (\text{A.11})$$

$$\mathbf{V}(\hat{\tau}_{\text{GAM}}) = \mathbf{q}^\top \mathbf{V}(\hat{\boldsymbol{\theta}}) \mathbf{q}, \quad (\text{A.12})$$

$$\text{Bias}(\hat{\boldsymbol{\theta}}) = -\tilde{\mathbf{H}}(\lambda_n)^{-1} \begin{bmatrix} 0 \\ -\frac{1}{n} Q_m(\lambda_n) \boldsymbol{\beta}_0 - \frac{\gamma_n}{n} \boldsymbol{\beta}_0 \\ 0 \end{bmatrix} = O\left(\frac{\lambda_n K_n^{1-m}}{n}\right) + o\left(\frac{K_n}{n}\right),$$

$$\mathbf{V}(\hat{\boldsymbol{\theta}}) = \mathbb{V}\left(\hat{\boldsymbol{\theta}} - \boldsymbol{\theta}_0 | S = 1\right) = \frac{1}{n} \tilde{\mathbf{H}}(\lambda_n)^{-1} \tilde{\mathbf{B}} \left\{ \tilde{\mathbf{H}}(\lambda_n)^{-1} \right\}^\top = O\left(\frac{K_n}{n}\right).$$

Step 4: We give the asymptotic normality of the difference $(\tau - \tau_0)$.

By Taylor expansion and Lemma B2, we have

$$\begin{aligned}
\tau - \tau_0 &= \mathbb{E} \{ \text{expit}(\tilde{\eta}(T = 1, X)) - \text{expit}(\tilde{\eta}(T = 0, X)) \} \\
&\quad - \mathbb{E} \{ \text{expit}(\eta_0(T = 1, X)) - \text{expit}(\eta_0(T = 0, X)) \} \\
&= \mathbb{E} \{ \text{expit}'(\tilde{\eta}(T = 1, X)) (\tilde{\eta}(T = 0, X) - \eta_0(T = 0, X)) \} \\
&\quad - \mathbb{E} \{ \text{expit}'(\tilde{\eta}(T = 0, X)) (\tilde{\eta}(T = 0, X) - \eta_0(T = 0, X)) \} \\
&\quad + o(\mathbb{E} \{ \tilde{\eta}(T = 0, X) - \eta_0(T = 0, X) \}) \\
&= \mathbb{E} \{ [\text{expit}'(\tilde{\eta}(T = 1, X)) - \text{expit}'(\tilde{\eta}(T = 0, X))] (\tilde{\eta}(T = 0, X) - \eta_0(T = 0, X)) \} \\
&\quad + o(\mathbb{E} \{ \tilde{\eta}(T = 0, X) - \eta_0(T = 0, X) \}) \\
&= \mathbb{E} \{ [\text{expit}'(\tilde{\eta}(T = 1, X)) - \text{expit}'(\tilde{\eta}(T = 0, X))] b_a(X) \} + o(\mathbb{E} \{ b_a(X) \}) \\
&= O(K_n^{-(p+1)}).
\end{aligned}$$

We denote

$$\text{Bias}_a(\hat{\tau}_{\text{GAM}}) = \mathbb{E} \{ [\text{expit}'(\tilde{\eta}(T = 1, X)) - \text{expit}'(\tilde{\eta}(T = 0, X))] b_a(X) \}. \quad (\text{A.13})$$

where $b_a(X)$ is given in (A.7). Finally we obtain that bias of $(\hat{\tau}_{\text{GAM}} - \tau)$, which equals to

$$\text{Bias}(\hat{\tau}_{\text{GAM}}) = \text{Bias}_a(\hat{\tau}_{\text{GAM}}) + \text{Bias}_\lambda(\hat{\tau}_{\text{GAM}}), \quad (\text{A.14})$$

with $\text{Bias}_\lambda(\hat{\tau}_{\text{GAM}})$ given in (A.11) and $\text{Bias}_a(\hat{\tau}_{\text{GAM}})$ given in (A.13).

To conclude, the bias of $\hat{\tau}_{\text{GAM}}$ can be bounded as

$$\text{Bias}(\hat{\tau}_{\text{GAM}}) = O(\lambda_n K_n^{1-m}/n + K_n^{-(p+1)}) + o(K_n/n).$$

Furthermore,

$$\mathbf{V}(\hat{\tau}_{\text{GAM}}) = O(K_n/n).$$

Thus we have mean squared error of $\hat{\tau}_{\text{GAM}}$:

$$\text{MSE}(\tau_{\hat{\text{GAM}}}) = O(K_n/n + K_n^{-2(p+1)}).$$

By setting $K_n = O(n^{1/(2p+3)})$ and $\lambda_n = O(n^v)$, where $v \leq (p+m+1)/(2p+3)$, we obtain the smallest order of MSE, which is $O(n^{-(2p+2)/(2p+3)})$. Thus we finish the proof.

A.3.5 Proof of Lemmas.

Next we give the proof of the two lemmas above.

Proof of Lemma B1: It is worth mentioning that our link function, denoted as $h(\eta)$, exhibits properties similar to the logistic link function. Therefore, the proof for Lemma B1 closely resembles that of Lemma A.4 in the reference paper Yoshida and Naito (2014), as well as Lemma A.1 to A.3 in Yoshida and Naito (2014).

Proof of Lemma B2: Barrow and Smith (1978) showed that there exists $\boldsymbol{\beta}^* \in \mathbb{R}^{D(K_n+p)+1}$ such that

$$\sup_{\mathbf{x} \in (0,1)^D} |\tilde{\eta}(\mathbf{x}) + b_a(\mathbf{x}) - \mathbf{Z}^\top \boldsymbol{\beta}^*| = o(K_n^{-(p+1)})$$

Where $\boldsymbol{\beta}^* = \left((\mathbf{b}^*)^\top, a^* \right)$. Let

$$\eta^*(\mathbf{x}) = Ta^* + \sum_{j=1}^D \eta_j^*(x_j) = Ta^* + \sum_{j=1}^D \mathbf{B}(x_j)^\top \mathbf{b}_j^*,$$

and

$$\eta_0(\mathbf{x}) = Ta_0 + \sum_{j=1}^D \eta_{j0}(x_j) = Ta_0 + \sum_{j=1}^D \mathbf{B}(x_j)^\top \mathbf{b}_{j0}$$

Since the asymptotic orders of $\eta_0(\mathbf{x}) - \eta^*(\mathbf{x})$ and that of $\boldsymbol{\beta}_0 - \boldsymbol{\beta}^*$ are the same, if $\boldsymbol{\beta}_0 - \boldsymbol{\beta}^* = o(K_n^{-(p+1)} \mathbf{1})$, we obtain for any $\mathbf{x} \in (0,1)^D$, $|\eta_0(\mathbf{x}) - \eta^*(\mathbf{x})| = o(K_n^{-(p+1)})$ hence Lemma B2 holds. Now we turn to prove that:

$$\boldsymbol{\beta}_0 - \boldsymbol{\beta}^* = o(K_n^{-(p+1)} \mathbf{1})$$

From the definition of $\boldsymbol{\beta}_0$, we have

$$\mathbb{E} \left[\log \frac{f(Y_1 | \mathbf{X}, \tilde{\eta})}{f(Y_1 | \mathbf{X}, \boldsymbol{\beta}_0)} \middle| S = 1 \right] \leq \mathbb{E} \left[\log \frac{f(Y_1 | \mathbf{X}, \tilde{\eta})}{f(Y_1 | \mathbf{X}, \boldsymbol{\beta}^*)} \middle| S = 1 \right] \quad (\text{A.15})$$

Since $b_a(x) = O(K_n^{-(p+1)})$ and $\frac{h'(\tilde{\eta}(x))^2}{V(h(\tilde{\eta}(x)))}$ is bounded, through the Taylor expansion, we have

$$\begin{aligned} \mathbb{E} \left[\log \frac{f(Y_1 | \mathbf{X}, \tilde{\eta})}{f(Y_1 | \mathbf{X}, \boldsymbol{\beta}^*)} \middle| S = 1 \right] &= \mathbb{E} \left\{ \mathbb{E} \left[\log \frac{f(Y_1 | \mathbf{X}, \tilde{\eta})}{f(Y_1 | \mathbf{X}, \boldsymbol{\beta}^*)} \middle| \mathbf{X}, S = 1 \right] \middle| S = 1 \right\} \\ &= \frac{1}{2} \mathbb{E} \left[\{ \tilde{\eta}(\mathbf{X}) - \eta^*(\mathbf{X}) \}^2 \frac{h'(\tilde{\eta}(\mathbf{X}))^2}{V(h(\tilde{\eta}(\mathbf{X})))} (1 + o_p(1)) \middle| S = 1 \right] \\ &= O(K_n^{-2(p+1)}), \end{aligned} \quad (\text{A.16})$$

and

$$\begin{aligned}
\mathbb{E} \left[\log \frac{f(Y_1 | \mathbf{X}, \tilde{\eta})}{f(Y_1 | \mathbf{X}, \beta_0)} | S = 1 \right] &= \mathbb{E} \left\{ \mathbb{E} \left[\log \frac{f(Y_1 | \mathbf{X}, \tilde{\eta})}{f(Y_1 | \mathbf{X}, \beta_0)} | \mathbf{X}, S = 1 \right] | S = 1 \right\} \\
&= \frac{1}{2} \mathbb{E} \left[\left\{ \tilde{\eta}(\mathbf{X}) - \eta_0(\mathbf{X}) \right\}^2 \frac{h'(\tilde{\eta}(\mathbf{X}))^2}{V(h(\tilde{\eta}(\mathbf{X})))} (1 + o_p(1)) | S = 1 \right] \\
&= \frac{1}{2} \mathbb{E} \left[\left\{ \tilde{\eta}(\mathbf{X}) - \mathbf{Z}^\top \beta_0 \right\}^2 \mathbf{C} | S = 1 \right], \tag{A.17}
\end{aligned}$$

where $\mathbf{C} = \frac{h'(\tilde{\eta}(\mathbf{X}))^2}{V(h(\tilde{\eta}(\mathbf{X})))} (1 + o_p(1))$. With (A.15-A.17), we obtain $|\tilde{\eta}(x) - \eta_0(x)| = o(1)$.

Since β_0 is the minimiser of $\frac{1}{2} \mathbb{E} \left[\left\{ \tilde{\eta}(\mathbf{X}) - \mathbf{Z}^\top \beta_0 \right\}^2 \mathbf{C} | S = 1 \right]$, we have:

$$\mathbb{E} [\mathbf{ZCZ}^\top \beta_0 - \mathbf{ZC}\tilde{\eta}(\mathbf{X}) | S = 1] = 0.$$

Furthermore, from the definition of β^* , we have

$$\tilde{\eta}(\mathbf{X}) = \mathbf{Z}^\top \beta^* - b_a(\mathbf{X}) + o_p(K_n^{-(p+1)}).$$

Hence, we obtain

$$\mathbb{E} [\mathbf{ZCZ}^\top (\beta^* - \beta_0) - \mathbf{ZC}b_a(\mathbf{X}) + \mathbf{ZC}o_p(K_n^{-(p+1)}) | S = 1] = 0.$$

The k -th component of first $(K_n + p)$ block of $\mathbb{E} [\mathbf{ZC}b_a(\mathbf{X}) | S = 1]$ is

$$\begin{aligned}
&\mathbb{E} [\mathbf{ZC}b_a(\mathbf{X}) | S = 1]_k \\
&= \sum_{j=1}^D \int_{[0,1]^D} \frac{h'(\tilde{\eta}(x))^2}{h(\tilde{\eta}(x))(1-h(\tilde{\eta}(x)))} B_{-p+k}(x_j) b_{j,a}(x_j) dP(x) (1 + o(1)) \\
&= o(K_n^{-(p+2)}).
\end{aligned}$$

The last equality can be obtained by mimicking the proof of Proposition 3.1 in Yoshida and Naito (2014). It can be also derived that $\mathbb{E} \{\mathbf{ZC}\} = O(K_n^{-1}\mathbf{1})$. Hence we have

$$\begin{aligned}
&\mathbb{E} [\mathbf{ZCZ}^\top (\beta^* - \beta_0) - \mathbf{ZC}b_a(\mathbf{X}) + \mathbf{ZC}o_p(K_n^{-(p+1)}) | S = 1] \\
&= \mathbb{E} [\mathbf{ZCZ}^\top (\beta^* - \beta_0) | S = 1] + o(K_n^{-(p+2)}) = 0.
\end{aligned}$$

Since $E[\mathbf{ZCZ}^\top | S = 1] = O(K_n^{-1}\mathbf{1}\mathbf{1}^\top)$. We have

$$\beta_0 - \beta^* = o(K_n^{-(p+1)}\mathbf{1}).$$

APPENDIX B. SUPPLEMENTS FOR THE NUMERICAL STUDIES IN SECTIONS 3-5

[Figure 4 about here.]

[Figure 5 about here.]

[Table 4 about here.]

[Table 5 about here.]

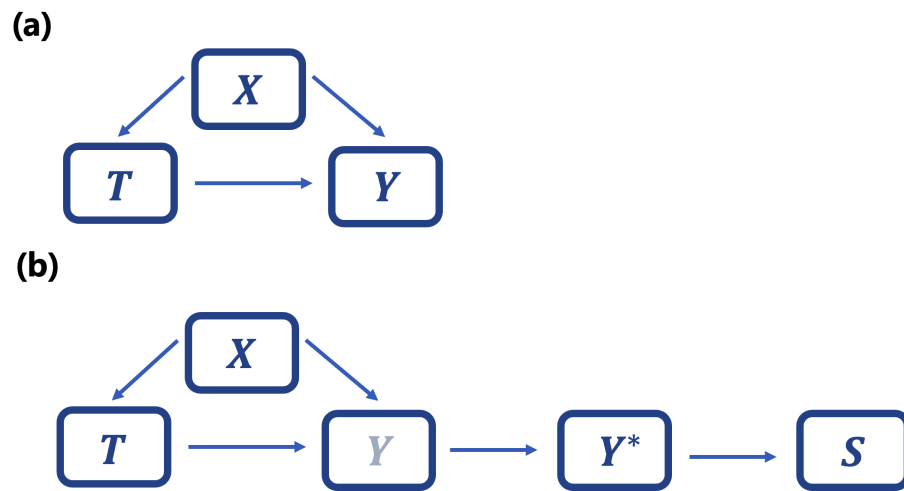


Figure 1. Causal directed acyclic graph (a) is the usual causal inference framework, while (b) is the ODS design with the mismeasured outcomes. The light color indicates the latent variable, and the dark color indicates the observed variables.

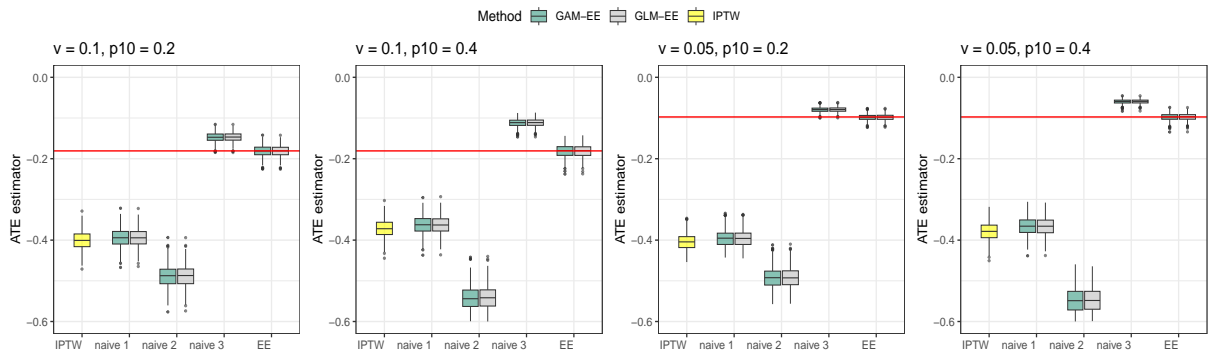


Figure 2. Estimators of τ under model **M1**. The red line is the true value of τ . naive 3 estimators are the EE methods ignoring the measurement information; naive 2 estimators are the EE methods ignoring the selection information; naive 1 estimators are the EE methods ignoring both selection and measurement information.

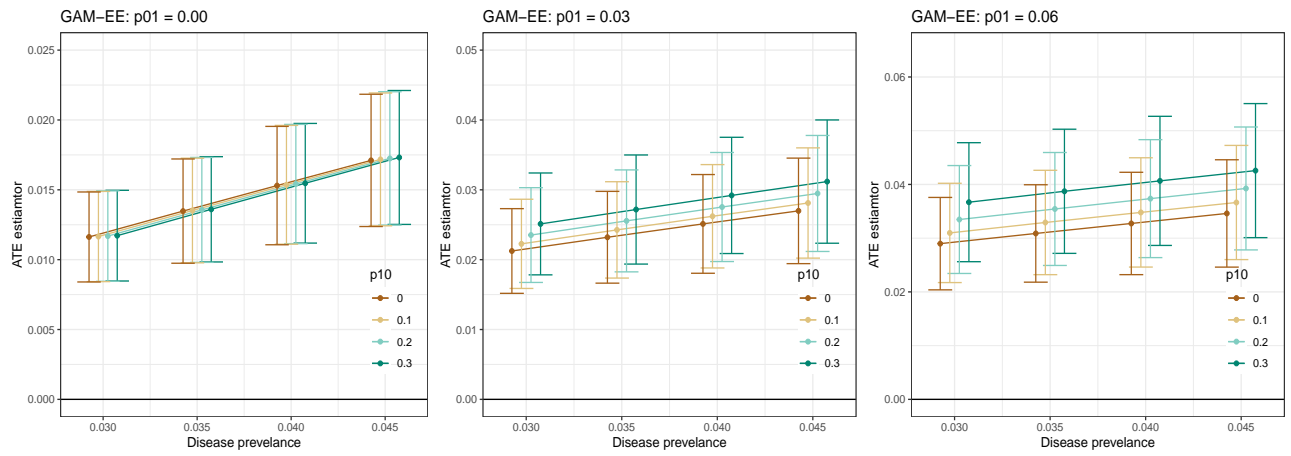


Figure 3. $\hat{\tau}_{\text{GAM}}$ and its 95% confidence interval in the sensitivity analysis of the UK biobank dataset.

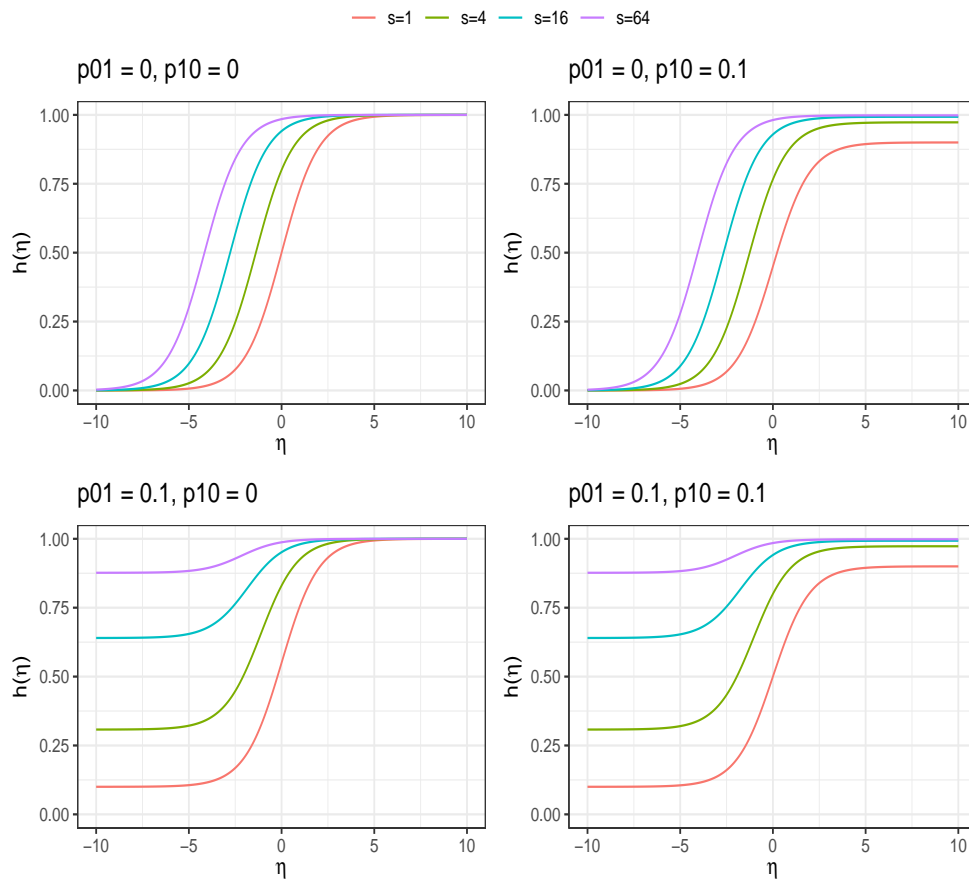


Figure 4. The shape of adjusted link function $h(\eta)$ under different p_{01} , p_{10} and s .

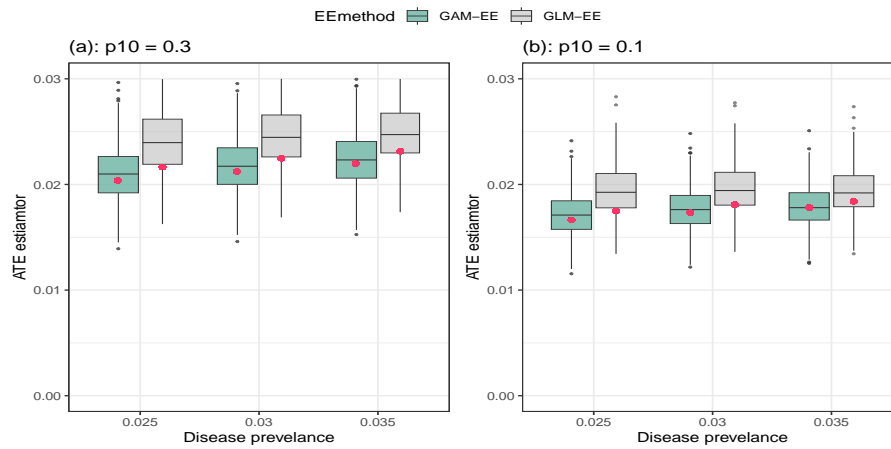


Figure 5. Estimators of τ under different predetermined disease prevalence and false negative rates. The red solid points are the benchmarks of the standard EE methods applied in the full dataset from UK biobank.

Table 1
Summary of simulation results for M1.

		<i>n</i> =500						<i>n</i> =2000					
<i>p</i> ₁₀	<i>v</i>	GAM-EE			GLM-EE			GAM-EE			GLM-EE		
		Rbias	RMSE	CP	Rbias	RMSE	CP	Rbias	RMSE	CP	Rbias	RMSE	CP
0	0.001	1.72	0.023	95.6	1.51	0.022	95.0	-0.14	0.011	94.4	-0.19	0.011	94.8
	0.01	1.60	0.218	95.4	1.49	0.214	95.2	0.58	0.105	95.2	0.48	0.104	95.2
	0.1	1.02	1.602	94.2	0.84	1.598	94.2	0.04	0.781	96.0	-0.02	0.780	96.2
0.2	0.001	1.58	0.022	95.4	1.50	0.022	95.8	0.40	0.010	94.8	0.37	0.010	94.6
	0.01	1.61	0.215	95.6	1.40	0.212	96.2	0.82	0.103	95.8	0.74	0.102	95.4
	0.1	1.44	1.695	95.0	1.31	1.683	95.2	0.19	0.819	95.2	0.18	0.817	95.6
0.4	0.001	1.93	0.022	95.8	1.70	0.022	96.6	0.64	0.012	93.4	0.60	0.012	92.8
	0.01	2.19	0.237	94.2	1.95	0.231	94.6	0.86	0.108	93.6	0.80	0.107	94.0
	0.1	0.57	1.711	96.0	0.57	1.712	95.6	0.28	0.819	95.8	0.26	0.818	96.2

Rbias, relative bias (%); RMSE, root mean squared error ($\times 1000$); CP, coverage probability (%).

Table 2
Summary of simulation results for M2 and M3.

model	p_{10}	v	$n=500$						$n=2000$					
			GAM-EE			GLM-EE			GAM-EE			GLM-EE		
			Rbias	RMSE	CP	Rbias	RMSE	CP	Rbias	RMSE	CP	Rbias	RMSE	CP
M2	0	0.001	-0.22	0.027	95.6	-6.04	0.027	88.6	-1.92	0.016	91.0	5.59	0.020	92.6
		0.01	0.44	0.236	95.4	-1.84	0.241	93.8	-1.16	0.134	94.6	5.02	0.167	90.0
		0.1	0.85	1.559	96.0	4.76	1.816	92.4	-0.13	0.749	94.8	-0.05	0.764	94.6
	0.2	0.001	0.19	0.027	95.8	-5.06	0.026	90.0	-1.10	0.017	94.0	5.79	0.021	91.0
		0.01	0.73	0.249	94.0	-1.52	0.242	94.2	-0.64	0.130	95.2	6.11	0.179	86.6
		0.1	0.94	1.658	94.2	4.93	1.916	92.8	-0.49	0.755	95.0	0.72	0.748	96.6
	0.4	0.001	0.18	0.028	94.8	-5.26	0.027	88.6	-1.25	0.016	94.2	6.13	0.020	92.4
		0.01	1.36	0.257	93.6	-1.07	0.250	94.0	-1.00	0.127	94.4	5.99	0.173	90.4
		0.1	1.00	1.521	96.8	5.40	1.830	95.2	-0.70	0.802	94.0	1.00	0.829	93.4
M3	0	0.001	0.52	0.025	95.4	17.94	0.048	83.4	0.10	0.012	94.2	16.30	0.037	34.2
		0.01	0.33	0.241	95.8	12.27	0.358	86.0	-0.16	0.118	94.2	10.71	0.251	58.4
		0.1	-0.00	1.587	94.0	-1.75	1.529	93.6	-0.08	0.804	94.4	-2.77	0.871	90.6
	0.2	0.001	0.41	0.025	95.4	18.05	0.049	86.8	-0.09	0.012	94.8	16.14	0.036	37.0
		0.01	0.19	0.231	94.8	12.78	0.357	88.6	-0.67	0.115	94.6	10.90	0.253	55.2
		0.1	-0.46	1.609	96.4	-1.01	1.534	95.6	-0.29	0.836	94.6	-1.67	0.838	92.0
	0.4	0.001	0.22	0.025	93.4	17.65	0.048	86.0	0.03	0.012	95.4	16.35	0.037	34.4
		0.01	0.13	0.228	95.2	12.93	0.356	87.6	0.06	0.112	95.6	12.00	0.270	52.4
		0.1	-1.71	1.853	93.0	-1.22	1.740	93.2	-0.15	0.855	94.8	-0.83	0.786	95.2

Rbias, relative bias (%); RMSE, root mean squared error ($\times 1000$); CP, coverage probability (%).

Table 3
Summary of simulation results for M4.

		<i>n</i> =500						<i>n</i> =2000					
<i>p</i> ₁₀	<i>v</i>	GAM-EE			GLM-EE			GAM-EE			GLM-EE		
		Rbias	RMSE	CP	Rbias	RMSE	CP	Rbias	RMSE	CP	Rbias	RMSE	CP
0	0.001	-0.68	0.031	91.8	6.27	0.033	95.2	0.16	0.014	96.0	5.69	0.018	90.8
	0.01	-1.54	0.248	93.8	5.96	0.278	95.0	-0.20	0.121	95.6	5.46	0.164	88.6
	0.1	-1.09	1.549	94.0	1.49	1.550	94.0	-1.06	0.757	93.8	-0.76	0.752	95.4
0.2	0.001	0.13	0.029	94.4	6.88	0.032	97.4	0.54	0.014	95.4	5.74	0.019	91.8
	0.01	-1.02	0.254	93.6	7.16	0.304	93.8	-0.01	0.123	95.0	5.71	0.168	88.2
	0.1	-1.35	1.535	94.0	2.68	1.665	93.8	-0.83	0.784	94.6	2.32	0.851	94.4
0.4	0.001	0.20	0.030	94.2	7.40	0.034	96.2	0.02	0.014	95.2	5.38	0.018	92.0
	0.01	-0.89	0.254	94.2	7.47	0.309	93.8	-0.27	0.127	95.0	6.00	0.173	87.0
	0.1	-2.10	1.553	95.0	3.04	1.654	95.8	-1.30	0.779	95.2	2.60	0.863	95.6

Rbias, relative bias (%); RMSE, root mean squared error ($\times 1000$); CP, coverage probability (%).

Table 4
Summary of simulation results for $p_{01} > 0$.

model	p_{10}	v	$p_{01} = 0.03$						$p_{01} = 0.06$					
			GAM-EE			GLM-EE			GAM-EE			GLM-EE		
			Rbias	RMSE	CP	Rbias	RMSE	CP	Rbias	RMSE	CP	Rbias	RMSE	CP
M1	0	0.05	0.25	0.538	95.4	0.24	0.538	95.2	-0.85	0.647	95.2	-5.59	0.833	87.4
		0.1	0.42	0.781	96.4	0.50	0.781	95.6	-0.74	0.869	94.8	-0.49	0.913	95.4
	0.2	0.05	0.25	0.586	95.6	0.23	0.593	95.4	-0.64	0.76	94.6	-6.64	0.994	85.0
		0.1	0.25	0.868	94.4	0.39	0.875	94.2	-1.39	0.982	93.2	-1.28	1.109	94.2
	0.4	0.05	0.40	0.639	95.8	0.32	0.642	95.8	-1.28	0.889	94.2	-9.23	1.248	85.8
		0.1	0.17	0.964	95.6	0.41	0.973	95.8	-2.61	1.231	93.0	-3.00	1.319	92.6
M2	0	0.05	0.10	0.519	95.2	-1.21	0.540	94.8	0.11	0.673	94.2	-5.95	0.865	86.0
		0.1	-0.35	0.703	96.8	1.80	0.794	95.2	-0.20	0.927	93.2	-0.64	0.952	93.8
	0.2	0.05	0.23	0.596	94.8	-2.18	0.631	92.6	0.85	0.793	92.0	-6.85	1.017	84.2
		0.1	-0.64	0.833	94.2	1.36	0.924	93.8	-0.03	0.974	95.4	-0.95	1.031	94.2
	0.4	0.05	0.21	0.681	95.4	-3.79	0.760	92.2	2.34	0.959	93.5	-8.15	1.198	86.2
		0.1	-0.73	0.961	94.4	0.82	1.011	94.6	-0.36	1.199	95.2	-2.07	1.277	92.4
M3	0	0.05	-0.19	0.538	94.4	2.35	0.600	93.2	2.28	0.684	93.8	4.59	0.792	90.2
		0.1	-0.38	0.741	95.8	-0.27	0.751	96.0	0.40	0.891	94.0	1.27	0.912	93.8
	0.2	0.05	0.05	0.561	95.2	3.46	0.671	92.6	1.84	0.725	95.0	4.77	0.870	92.2
		0.1	-0.48	0.864	93.6	0.99	0.888	94.2	0.76	1.013	95.2	3.20	1.177	91.2
	0.4	0.05	1.01	0.642	95.0	5.05	0.823	90.2	2.75	0.911	93.8	5.53	1.061	91.6
		0.1	-0.89	0.975	94.0	1.78	1.023	94.8	0.69	1.102	95.6	4.17	1.345	91.8
M4	0	0.05	-1.69	0.522	94.4	0.84	0.524	95.4	0.26	0.615	94.0	-0.15	0.646	93.2
		0.1	-1.14	0.760	93.4	1.14	0.817	94.4	-0.06	0.830	95.8	1.17	0.874	95.2
	0.2	0.05	-2.27	0.573	92.4	0.69	0.598	95.4	-1.19	0.707	94.8	-1.50	0.767	93.8
		0.1	-2.73	0.862	90.4	0.82	0.834	95.8	-1.21	0.939	95.0	1.16	0.994	94.8
	0.4	0.05	-1.88	0.634	94.4	1.15	0.676	95.2	0.58	0.790	95.8	-0.39	0.864	96.4
		0.1	-2.49	0.942	92.6	2.02	0.958	95.2	-1.37	1.075	95.2	1.65	1.165	96.4

Rbias, relative bias (%); RMSE, root mean squared error ($\times 1000$); CP, coverage probability (%).

Table 5*Demographic and lifestyle characteristics of 136741 persons by Alcohol Intake Category in the UK Biobank Study*

	Overall	Non-consumer	Consumer	p-value
n	136,741	63,478	73,263	
gout = 1 (%)	5264 (3.8)	2010 (3.2)	3254 (4.4)	<0.001
edu = 1 (%)	49242 (36.0)	19530 (30.8)	29712 (40.6)	<0.001
ethnicity = 1 (%)	125352 (91.7)	57022 (89.8)	68330 (93.3)	<0.001
TDI = 1 (%)	68370 (50.0)	34189 (53.9)	34181 (46.7)	<0.001
exercise = 1 (%)	68345 (50.0)	31798 (50.1)	36547 (49.9)	0.446
diet score (mean (SD))	-0.61 (1.03)	-0.56 (1.07)	-0.65 (1.00)	<0.001
age (mean (SD))	57.13 (8.06)	56.37 (8.37)	57.78 (7.72)	<0.001
household income (mean (SD))	2.69 (1.19)	2.49 (1.16)	2.86 (1.18)	<0.001
BMI (mean (SD))	27.84 (4.14)	28.20 (4.45)	27.52 (3.84)	<0.001

gout (coded as 1 for diagnosed with gout); edu (coded as 1 for college education and 0 for others); ethnicity (coded as 1 for White ethnicity and 0 for others); TDI (Discrete Townsend Deprivation Index, with TDI coded as 1 for the top 50% individuals and 0 for others); exercise (coded as 1 for individuals in the top 50% of daily exercise time and 0 for others); diet score (a measure of healthy diet adherence); household income (classified into ordered discrete categories: 1 for less than 18,000, 2 for 18,000 to 30,999, 3 for 31,000 to 51,999, 4 for 52,000 to 100,000, and 5 for greater than 100,000); BMI (calculated as weight divided by height squared);